AN ASSESSMENT OF THE IMPACT OF HARMATTAN PARTICLES ON MICROWAVE PROPAGATION IN THE SAVANNAH REGION (A CASE STUDY OF N'DJAMENA, CHAD)

BY

NALDONGAR PARFAIT

A THESIS PRESENTED TO THE DEPARTMENT OF ELECTRICAL ENGINEERING AHMADU BELLO UNIVERSITY, ZARIA IN PARTIAL FULFILLMENT OF THE REQUIREMENTS FOR THE AWARD OF THE DEGREE OF MASTER OF SCIENCE (MSc) IN ELECTRICAL ENGINEERING

SEPTEMBER, 2007

DECLARATION

I, Naldongar Parfait, hereby declare that this thesis in its entirety is based on my research under the supervision of Dr. Danjuma. Dajab and Dr. K. S. Farayola and has never been presented anywhere else in any form for any degree whatsoever.

All sources of information are specifically acknowledged by means of references.

---------- ----------

NALDONGAR Parfait
MSC/ENG/48221/2005-2006 **Date**

CERTIFICATION

This thesis entitled "**An assessment of the impact of Harmattan particles on microwave propagation in the savannah region: A CASE STUDY OF N'DJAMENA, CHAD**" meets the regulations governing the award of a master of science (M.Sc) Degree in electrical engineering of Ahmadu Bello University and is approved for its contribution to knowledge and literary presentation.

---------- ----------

Dr. D.D. Dajab **Date**

Main Supervisor

---------- ----------

Dr. K.S. Farayola **Date**

Minor supervisor

---------- ----------

Dr. M. B. Muazu

Head of Department **Date**

---------- ----------

Professor S.A. Nkom.

Dean, Postgraduate School **Date**

DEDICATION

This thesis is dedicated to: Almighty God

Naldongar Ali Ernest,

Eldjiman Cecile,

Naldongar Beldene Madeleine

for their love, understanding and care during the course of this thesis

ACKNOWLEDGEMENT

"You, Lord, are all I have, and you give me all I need, my future is in your hands" (Psalm 16:5).

I want to acknowledge the grace and power of God Almighty that has been upon me since my birth, for he has always ordered my steps in accordance with God's will, up to this point in my academic pursuit and may his will be done.

Any work represents the integrated educational background and experience of the author. I wish to thank all those who provided the environment and motivation for me to acquire the knowledge necessary for this effort. Special thanks go to two academic experts, Dr D. Dajab and Dr.K.S.Farayola that put me through challenges and encouraged me. For Dr D.D Dajab I want to thank him for his good supervision, guidance, encouragement and advice which have contributed immensely to the successful completion of this thesis. Academic Dr K. S. Farayola I want to thank him for his good supervision, encouragement and advice which have contributed immensely to the successful completion of this thesis.

I am particularly grateful to another academic and industry expert professor B.G Bajoga whose academic and research experience has greatly contributed to the thesis.

Thank you, sir for your advice

I am particularly grateful to another academic giant very Rev. Fr (Dr) Joseph Haruna Mamman and Rev. Fr (Dr) Peter Tanko who have spiritually contributed to the Thesis Thank you, fathers, for your advice.

I am particularly grateful to the staff of electrical engineering department for their assistance.

I wish to also acknowledge all Chadian's students in Nigeria.

To my parents, I say thanks a million times for the sacrifices and deprivation they had to bear, for they toiled to make my life more comfortable than theirs. Words alone can never say thank you enough. To my friends: Kosmadji, Mbatina Theodore, and Ndorgoto Madjiadoum, I say thanks a million times for your sacrifices made towards me.

To my darling Miss Mbai-amdene Beatrice I greatly appreciate your support and encouragement.

God is about to do a great thing in return.

NALDONGAR PARFAIT

ABUDEE, Zaria

SEPTEMBER 2007.

ABSTRACT

This thesis reports the result of an assessment of the impact of harmattan particles on microwave signals in the savannah region. Emphasis was placed on the spatial harmattan particle density, the specific particle attenuation variation, the atmospheric attenuation and the dominant propagation mechanism during the harmattan period which is peculiar to the savannah region. The report studied scattering mechanism, absorption mechanism and specifically described how to determine the specific particle attenuation, atmospheric losses and spatial harmattan particles density. The attenuation of wavelengths in the 900MHz and 1800MHz band during harmattan period in the savannah region was studied and path loss curves are presented. The significant results obtained are also discussed and interpreted. Finally the comparative statistical analysis of the results has been done. It is established that the particle density is responsible for the scattering of electromagnetic energy which leads to attenuation in its signal strength. For the year 2004, the atmospheric losses range between 3.7dB and 12.55dB, for 2005, the atmospheric losses range between 3.3dB and 18.94dB for 2006, the atmospheric losses range between 1.71dB and 13.03dB. From the statistical analysis, the highest path loss occurs on Farcha road while the lowest occurs on Moursal road.

TABLE OF CONTENTS

LIST OF FIGURES

LIST OF TABLES

LIST OF ABBREVIATIONS/SYMBOLS

ITC: Inter-Topical Convergence

ITF: Inter-Topical Font

D: Electric Flux density

B: Magnetic Flux density

E: Electric Field

H: Magnetic Field

m: Dipole moment

I: Moment of inertia

E: Electromagnetic Field Strength

N_o: Number of dipoles per unit volume

ω_o: Angular Frequency of the electromagnetic Field

n: Number of pairs of observation

x: The Temperature of observation

y: Particle Size distribution

V_{fm}: The best visibility figure

V_i: Measured visibility profile

H: Humidity profile

V: Visibility

λ: Wavelength

σ: Atmospheric attenuation

ρ_p: Mean particle

a: Regression coefficient

b : Regression coefficient

q: The Size distribution of the Scattering Particles

α: The Specific particle attenuation variation

T_x: Transmitter antenna

R_x: Receiver antenna

S_R: Measured received signal strength

Lp: path loss

EIRP: effective isotropic radiated power

LOS: Line of sight

CHAPTER ONE

GENERAL INTRODUCTION

1.1 INTRODUCTION

It has been established that the impact of harmattan particles can lead to Ssssssatmospheric attenuation, signal fading, obstructions in the signal path and multipath effects leading to a drop in the signal power.[1] This thesis is aimed at the assessment of the impact of harmattan particles on microwave propagation in the savannah region with N'Djamena, Chad as a case study.

Chad is a continental country located in the northern hemisphere. The co-ordinates of Chad are: 8^0 latitude and 24^0 latitude (tropic of cancer for latitude North, 14 and 24 degree of longitude East). Its area is 1,284 million sqkm. Chad is a land locked country located in North Central Africa. It shares boundary with, Libya to the North, Sudan to the East, the Central African Republic to the South, Cameroon and Nigeria to the South West and Niger to the West. The country is mostly an arid, semi –desert plateau on the edge of the sahara desert. Its prominent feature is the broad shallow basin of Lake Chad in the South and South West part of the country, from there the land rises gradually to plateau in the South while to the North of the Basin the land rises to the Ennedi Plateau and the volcanic Tibesti Ranges. For the most part the country vegetation is generally desert scrub or steppe [2].

Chad is placed under the influence of the anticyclone of Libya (continental air: harmattan monsoon). These anticyclones provoke the motion of masses of air that push each other either in South-East direction or according to reverse direction. The Inter-

Topical Convergence zone (ITC) or the Inter-Topical Font (ITF) moves between 4^0 and 20^0 Latitude North according to the apparent motion of the sun.

Chad has three climatic zones:

(1) A Subtropical Zone within the equatorial rain belt to the South with a wet season from May to November and a dry season from September to April.

(2) A Sahelian Zone in the Central region which has a longer dry season and a brief wet season between June and September.

(3) The Saharan Zone in the Northern region which has a true desert climate with hot and arid conditions and is almost entirely rainless. Average annual precipitation in N'Djamena is 744mm (29 inches) and the average temperature ranges are from 14 to 35 degrees Celsius (57 to 91 degrees Fahrenheit) in December to 23 to 42 degrees Celsius (73 to 108 degrees Fahrenheit) in August. [2]

In Chad the harmattan season occurs between December and March.

1.2 THESIS MOTIVATION

Communication systems: such as radar system, radio navigation, heating, energy transfer, mobile communication, remote sensing, control and recording use microwave frequencies as a fundamental transmission medium for their operations.

The need for assessing the effect of harmattan on microwave propagation is for monitoring of the radio signals and measurements of their field strength and fading characteristics and analyses.

This investigation can also lead the radio planner to a thorough understanding of microwave propagation in the savannah region for designing point- to- point links among other things.

1.3 STATEMENT OF PROBLEM

It has been previously investigated and found that harmattan disturbs propagation of radio signals at frequencies generally above 30MHz. It is well known that radio reception in general and microwave signals in particular, are affected by the phenomenon of fading. The result is that, the incoming radio signal which enters the receiver circuitry varies in magnitude. These variations are attributed to changes in propagation conditions. In extreme cases it can even lead to complete cancellation of a signal at the receiving point. These signal variations can occur fast or slow and the speed at which they take place is known as “rate of fading” the reception of microwaves depends on their propagation between a transmitter and a receiver [3].

In the savannah region and hence also in N’Djamena capital of Chad, the atmosphere is seasonally affected by: “harmattan”; a weather condition during which dust is blown southwards from the sahara desert by a North East wind. Dust particles of about a micron size are finally deposited when the North East wind loses its speed on meeting a warm and opposite wind from the Gulf of Guinea. The intensity of the harmattan may be so great that the visibility at ground level is reduced to less than a hundred meters.

The main objective of this thesis is, therefore, to find out whether, and how, the harmattan is influencing microwave propagation in the region in general and N’Djamena in particular. To carry out this investigation, the records of ground level visibility during

harmattan will be analyzed with respect to the actual particle rate (or density) of harmattan dust in the air. On the strength of these analyses, specific attenuation during harmattan will be analysed and computed. After field strength measurements, the pathlosses in a typical case will be discussed.

1.4 THESIS OUTLINE

This thesis report begins with a general introduction of an assessment of the impact of harmattan particles on signals and the climate of Chad as contained in chapter one. This chapter also contains the basis for this research. In chapter two, literature review related to the theory of dielectrics and electrodynamics are discussed, and in chapter three, the methodology and data collection used in this work is presented. Chapter four contains the results obtained and the analysis. Interpretation of the results is also discussed in this chapter. Finally, chapter five rounds off with limitations, problems encountered and the solution proffered. It also contains conclusions and recommendations for further work.

CHAPTER TWO

LITERATURE REVIEW

2.0 INTRODUCTION

Continental sub-tropical climates correspond to the regions (latitude 10^0 and 20^0) where the climate is characterized by a dry winter and rainy summer are called savannah. In this region there are markedly daily and annual variations of radio propagation conditions with the least attenuation in the rainy season.

2.1 LITERATURE REVIEW

Dajab [1] conducted a study on characterisation and modelling of 900MHz in-door wireless communication channels in the savannah region, made an analysis on the impact of harmattan on UHF signals by relating the records of ground level visibility to the particle rate of harmattan dust in air. As resulted during harmattan period, multipath activity is increasing due to the presence of harmattan dust in the air as a result of the particle dynamics which coincide with the highest temperatures of the hours of the day. The greatest losses are not due to absorption in the particles themselves but to scattering which depends on relative values of the wave length and the size of the particles.

Neyman [3] in an indirect manner conducted a number of studies on the impact of harmattan on RF in the HF sub-band and for ionized media; He used photographic capture of the ground level visibility and relative humidity measurement to analyze electromagnetic field variation in the outdoor environment.

Isaac et al [13] conducted a work on comparison of laser beam propagation at 785nm and 1550nm in fog and haze for optical wireless communication and found 785nm, 850nm and 1550 light suffer from atmospheric attenuation. This observation is

based on an extensive literature search, and from full Mie scattering calculation. In order to achieve the high availability requirements of the telecommunications industry, laser communication links, will have to be short (<500m), or backed up by a redundant microwave or millimetre wave link at lower speed.

Fog, heavy snow, and extreme rain are the primary types of weather that can affect these short and laser communication links.

Dajab [14], Published information concerning the effect of harmattan on radio frequency waves.The work observed that harmattan dust clusters at their highest intensities can reduce visibility to less than hundred meters. The clusters consist predominantly of quartz layer which non coherently scatters RF signals. The power absorption and scattering during harmattan period increase rapidly with frequency and with density of the precipitation.

Alexandre, [15] conducted a study on a set of basis functions to improve numerical calculation of Mie scattering in the chandrase khar-sekera representation. The scattering of an electromagnetic plane wave by a spherical particle of arbitrary size is known as mie scattering.

Eyo, et al [16] conducted an investigation on microwave signal attenuation in harmattan weather. The measurement was made with the intent of highlighting microwave signal attenuation in harmattan weather conditions. This work shows that microwave LOS link in this region and regions with similar climatic characteristics is prone to signal degradation as well as fading in the harmattan season, and associated ailments..

Halit et al [17] worked on particles concentration characteristics and density measurements of slurries using electromagnetic flow meters. His results indicated that, as the particle's concentration increases, the generated signal amplitude decreases.

Hamilton et al [18] worked on this subject, discovered that harmattan dust storms or dust haze have had long desert track and are therefore very dry, hot by day and cool by night, and frequently are laden with dust. A microscopic examination of harmattan dust made at the Imperial Institute, London, showed that a considerable proportion of the dust is composed of diatoms of many different species, some entire but many of them fragmentary, together with particles of quartz, most of which are less than 0.025mm in diameter odd fragments of biotite and what appears to be riebeckite are also present, with a quantity of very fine dust, indeterminate microscopically, and vegetable tissues. The figure of 0.025mm gives an idea of the maximum values of the diameter and throws little light on the size of the particles which are most effective in absorbing or scattering the light and it is possible even likely, that it is the "quantity of very fine dust, indeterminate microscopically", consisting probably of large number of particles of the order of magnitude of wave length of light, that are mainly responsible for producing the haze.

Mohamed, [19] Conducted work on microwave and millimeter wave solution. He discovered that both are attenuated by atmospheric constituents and gases at different rates for different frequencies. Where gaseous absorption is at minimum are called atmospheric windows and regions of maximum absorption are called absorption bands.

SHITTU [20] worked on cellular mobile radio propagation characteristics. He conducted investigation on influence of obstacles on the propagation of EM waves.

Among those obstacles, atmospheric variation was included as one of the most important impairments that need to be included as an essential part of a realistic radio channel model such as path loss, multipath propagation and shadowing.

2.2 DIELECTRIC MATERIALS

Harmattan dust particles are reported to consist predominantly of small size dielectric materials like quartz. A dielectric material is one that is electrically insulating (non metallic) and exhibits or may be made to exhibit an electric dipole structure; that is, they are susceptible to polarization in the presence of an electric field [4]. Dielectric materials are of two types,

i. Piezoelectric materials which include titanates of barium, and lead, lead zircouate, ammonium dihydrogen phosphate and quartz. Polarization in these materials may be induced by an external electric field.

ii. Ferroelectric materials include Rochelle salt, potassium dihydrogen phosphate, etc. These materials exhibit spontaneous polarization, that is, polarization in the absence of an electric field [9]

Polarization is the alignment of permanent or induced atomic or molecular dipole moments with an externally applied electric field (that is, a separation of positive and negative electrically charged entities on a molecular or atomic level). These elements are reported to have a profound influence on the propagation characteristics of both RF and Microwave signals. The dominant propagation mechanisms are discussed in the following paragraphs:

2.3 ABSORPTION MECHANISM

It is expedient from the foregoing considerations that since the harmattan dust particles are continuous over the dielectric space, we may partition the domain (volume) into a number of vertical planes x = (x_1, x_2…….x_N) separated by intervals Δd. if the electric field E over some reference plane containing the 0 is E_o, the electric field E_i over a plane a distance nΔd away from the reference plane in the direction of propagation will be [5]

$$E_i = E_o \exp(-jkn\Delta d)v/m \text{ ----------(2.1)}$$

Where $K = \omega(\mu\varepsilon)\frac{1}{2}$ is the phase constant and shows by how much the phase of the plane wave is retarded in unit distance.

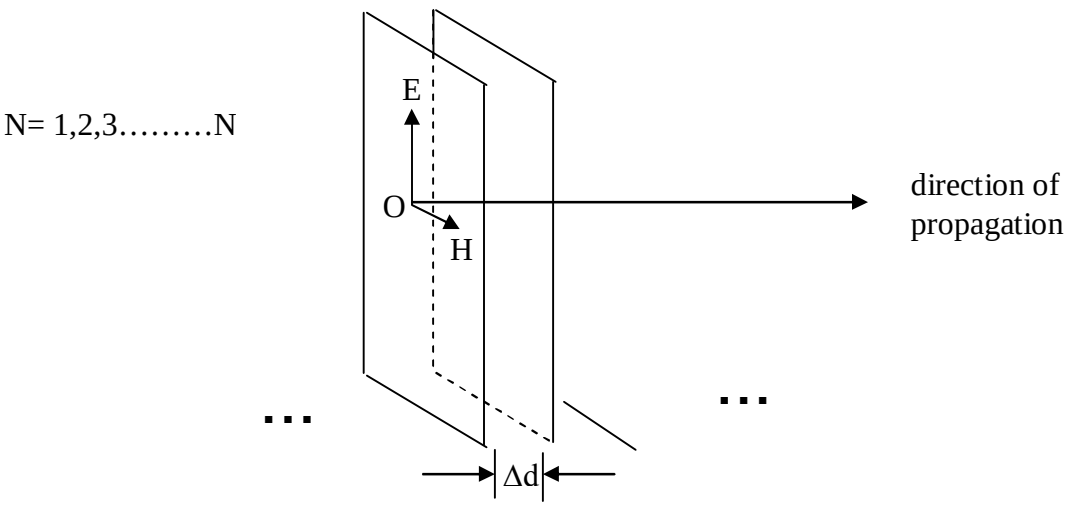

Fig. 2.1 Plane in the dielectric space

Maxwell's first equation for imperfectly conducting media is given as

$$\varepsilon\frac{\partial E}{\partial t} + \sigma E = \text{curl H A/m}^2 \text{ ----------(2.2)}$$

If the electric field varies in time harmonically, then

$$E = E_m e^{j\omega t} V/m. \quad \text{---------- (2.3)}$$

In terms of its time derivative

$$E = -\frac{j}{\omega}\frac{\partial E}{\partial t} V/m \quad \text{---------- (2.4)}$$

Substituting equation (2.4) into equation (2.2) yields

$$\left(\varepsilon - j\frac{\sigma}{\omega}\right)\frac{\partial E}{\partial t} = \text{curl H A/m}^2 \text{----------(2.5)}$$

Comparing equation (2.5) with, Maxwell's equation for an ideal dielectric which can be derived from (2.1) by putting ϭ = 0 such that

$$\varepsilon\frac{\partial E}{\partial t} = \text{curl H} \text{----------(2.6)}$$

We note that the complex quantity

$$\varepsilon_c = \varepsilon - j\frac{\sigma}{E} F/m \quad \text{---------- (2.7)}$$

is in effect the permittivity of an imperfectly conducting medium [1]. In calculations it is more convenient to use the relative (i.e dimensionless) complex permittivity or the complex dielectric constant which is obtained by dividing complex permittivity with ε_0.

$$\varepsilon^1 = \frac{\varepsilon_c}{\varepsilon_0} = \frac{\varepsilon}{\varepsilon_0} - j\frac{\sigma}{\omega\varepsilon_o}$$
$$= \varepsilon^1 - j\frac{\sigma\lambda 36\pi \times 10^9}{2\pi x}$$
$$= \varepsilon^1 - j60\lambda\sigma \quad \text{---------- (2.8)}$$

Where C = 3 x 10^8m/s; ε_0 = 8.854 x 10^{-12} F/m

From field theory it is known that the electric field of a radio wave propagated in an ideal dielectric is descried as

$$E_z E_m e^{j\omega}\left(t - \frac{d\sqrt{\varepsilon^1}}{c}\right) V/m \quad \text{----------} \quad (2.9)$$

Where ε' is the dielectric constant of an ideal dielectric expressed in equation (2.9) and may be extended to include an imperfectly conducting medium by replacing the real ε' with the complex expression of equation (2.8) by putting $\sqrt{\varepsilon'} = n - jp$ and substituting into equation (2.9). Doing this yields

$$E_z = E_m e^{\frac{\omega}{c} pd} \frac{j\omega}{e}\left(t - \frac{dn}{c}\right) V/m \quad \text{----------} \quad (2.10)$$

Equation (2.10) shows that propagation in an imperfect medium is accompanied by a reduction in the wave amplitude in an exponential fashion. The quality

$$\delta = \frac{\omega}{c} p\ m^{-1} \text{----------} (2.11)$$

is called the absorption coefficient and the velocity of waves in the imperfect medium is

$$V = \frac{c}{n} \quad \text{----------} \quad (2.12)$$

The harmattan dust filled space has the dielectric particles subjected to polarization by the electric field. The inducement of dipoles in the particles making up the volume of space absorb electrical energy as in equation (2.11) and the wave suffers attenuation as it proceeds. Generally the dipoles attempt to reorient with the field and for each polarization a minimum reorientation time exists which depends on the ease with which the particular dipoles are capable of realignment. A relaxation frequency is taken as the

reciprocal of this reorientation time, a dipole ceases to shift reorientation direction when the frequency of the external electromagnetic field exceed its relaxation frequency, and therefore will not make a contribution to the dielectric constant of the space that is when polarization mechanism ceases to function, there is an abrupt drop in the dielectric constant . Generally the contribution of the dipole to the space dielectric constant is [7]:

$$\Delta\varepsilon = \frac{2}{3}\frac{m^2 E N_0}{I\omega_o} \text{ ---------- ---------- ----------} \quad (2.13)$$

Where

m - dipole moment

I – moment of inertia

E – electromagnetic field strength

N_o – number of dipoles per unit volume

ω_o- angular frequency of the electromagnetic field

2.4 SCATTERING MECHANISM

Attenuation due to absorption is larger than attenuation due to scatter for wavelengths that are small compared with the particle size. For wavelengths that are long compared to the particle size, the attenuation due to scatter is larger than the attenuation due to absorption [8] the wavelength at 900MHz and 1800MHz which is fairly large relative to the sizes of the harmattan dust particles. In this circumstance, the mechanism of scattering is predominant. particles, taking into consideration the axiom on free-moving particles and the assumption concerning wind speed.

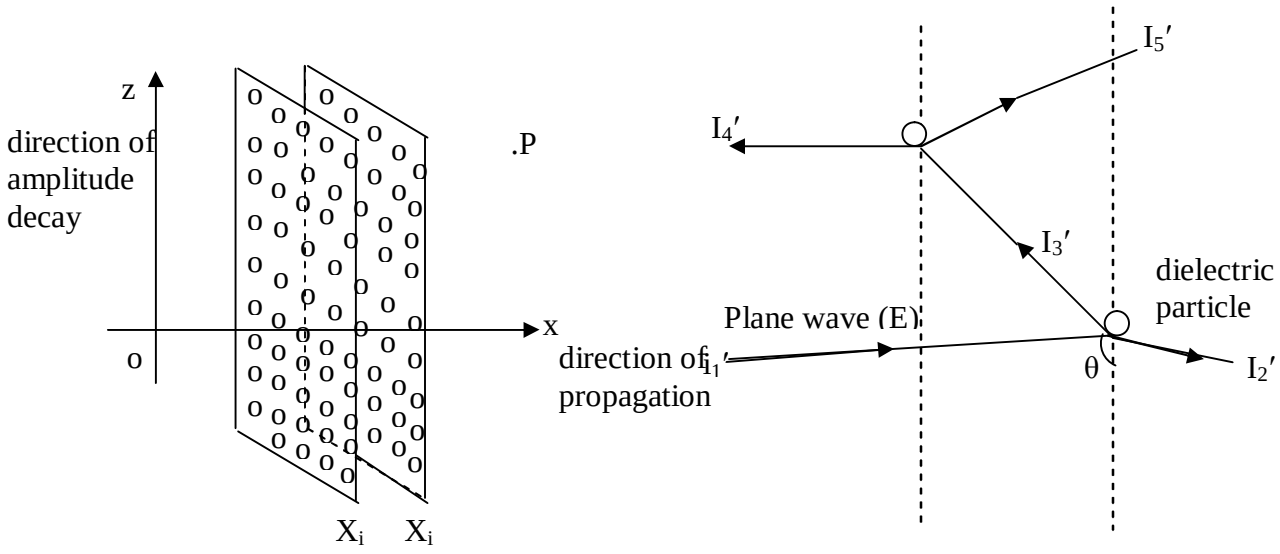

(a) Instantaneous diagram of scattering (b) Ray diagram of scatteing

Fig. 2. 2 Illustration of instantaneous and ray diagram of scattering

When the wavelength is large compared with the size of the particle, the wave is scattered in arbitrary or all directions, but when the wavelength is small compared with the particle size then most of the scattering takes place within a narrow cone surrounding the forward direction of propagation of the incident radiation [9]. In order to understand the physical phenomena of scattering, let us consider the elemental contribution to the x-component of the electric field. The vector position of a field p with respect to the origin is

$$r = a_x x + a_z z \quad (2.14)$$

Where a_x and a_z are unit vectors in the directions of the axes x and z. the unit vector in the direction of propagation of the plane wave is

$$a = a_x \cos\Phi - a_z \sin\Phi \quad \text{----------} \quad (2.15)$$

Where cosθ= c and sinθ =S are direction consines, the elemental contribution to the x – component is the contribution of that plane- wave in the spectrum of scattered waves traveling in the direction making an angle ϕ = cos-1C to the x – axis. When $|c| \leq 1$, ϕ lies in the range $\frac{\pi}{2} \leq \Phi \leq \frac{\pi}{2}$, the elemental plane wave is of the homogenous type. When $|c| > 1$, assuming c to be real, the character of the wave changes because.

$$S = \sqrt{(a - c^2)} = \pm jx \quad \text{----------} \quad (2.16)$$

Where x – which was real and positive, is now imaginary. As a result the plane wave becomes the in-homogenous type and the amplitude of the wave is no longer constant over planes of constant phase. This in-homogenous (scattered) plane wave has the following properties.

i. The direction of propagation of the wave is along the x – axis, that is parallel to the planes x_i and x_j, either positive or negative depending on the sign of c;

ii. The amplitude of the field components (scattered) decreases exponentially in the +z direction away from the planes x_i, x_j

The scattering of energy in arbitrary directions gives rise to a net loss of energy in the direction towards the receiver .

2.5 HARMATTAN PARTICULE DENSITY

The harmattan is a weather condition in the tropics in which dust particle (precipitates) are blown up into the air by winds defined as air in horizontal motion relative to the earth surface and pushed southwards from the Sahara desert by the northeast winds. Harmattan intensity may be so great that visibility at ground level is

reduced to less than a hundred meters by the dust clusters. Harmattan occurs in Chad during the dry season that is, between the months of November and March

Generally the problem of estimating the attenuation of RF waves caused by the various forms of precipitation like rain, snow, and harmattan dust etc) is quite difficult. In practice it has been convenient to express the attenuation due to rain as a function of the precipitation rate [10].

The interaction between water drops and radio waves cause an attenuation that, for a given rain rate depends on the size and shape of the raindrops. The effect of rain precipitation is usually expressed in terms of specific attenuation which is predicted with the aid of an empirical relationship given by [11]

$$\alpha_{rain} = a\rho^{b} dB/km \text{ ----------(2.17)}$$

Where ρ – the rainfall rate (mm/hr); a, b – regression coefficient which are a function of the frequency f, of the temperature T, of the drop size distribution and to a lesser extent, of the wave polarization.

In the case of harmattan, no known attempt at quantifying or measuring its precipitation rate is available except the measure of how it distracts visibility (with respect to distance) to fully understand the mechanism of harmattan attenuation therefore it is essential to estimate the rate of the harmattan precipitations.

By analogy to the attenuation of microwave signals (UHF: 300-3000MHz) and (SHF: 3-30 GHz) are collectively called microwave by rainfall, the specific attenuation due to harmattan dust particle may be predicted using the modified equation (2.17). Further experiments are required to establish the validity of this interpretation. Here the

coefficients a and b are function of frequency f, of temperature T, and of the particle size distribution. The problem of calculating the value of a and b for a given meteorological data is given by the relations [12]

$$b = \frac{n\left(\sum_{i-1}^{n} x_i y_i\right) - \left(\sum_{i=1}^{n} xi\right)\left(\sum_{i=1}^{n} yi\right)}{n\left(\sum_{i=1}^{n} {x_i}^2\right) - \left(\sum_{i=1}^{n} x_i\right)^2} \text{----------(2.18)}$$

$$a = \frac{\sum_{i=1}^{n} y_i - b\sum_{i=1}^{n} x_i}{n}$$

Where n – is the number of pairs of observation;

x – is the temperature of observations; and

y – particle size distributions.

Available meteorological data on harmattan dust, however, are currently presented in terms of visibility in units of distance and the question is how to relate these records of ground level visibility to the actual particle rate (or density) of harmattan dust in the air. It is known that a pressure increase and a temperature decrease are responsible for the movement of wind, which serve as a means of transporting heat, dust particle, moisture etc [13] here a spatial particle density ρ [g/m3] may be a meaningful concept given that the dust particle carrying capacity of the winds depend on the relative humidity.

The spatial harmattan particle density may be approximated by the empirical relation

$$\rho_i = \frac{(V_{fm} - V_i)\rho_p}{h} g/m^3 \quad \text{----------(2.19)}$$

Where Vf_m- the best visibility figure for the year (period) [m];

V_i – observed (measured) visibility profile[m];

ρ_p- mean particle density [g/m^3]; and

h- humidity profile (in decimals) [g/m^3].

From the record of monthly meteorological observations, obtained from the Meteorological Department of N'Djamena (Chad) ASECNA, the mean temperature, minimum temperature, maximum temperature and the estimated density of harmattan dust for the period of study are as presented in chapter four. (Calculated by assuming the mean particle density to be equivalent to the mean particle density in contaminated water= $0.889 \pm 0.01 g/m^3$) [14].

If we assume a state in which the harmattan dust particle consists of a subset of the complete set of fixed sizes (which have small details compared to the wavelength) and with a certain distribution per cubic meter (which may be ascertained experimentally), then we may obtain using the adopted equation (2.17), the specific particle attenuation variation in dB/m, as: $\alpha_{particle} = a\rho_b$.

The power absorption and scattering by these particles (hamattan dust, fog etc) increase rapidly with frequency and with density of the precipitation. The greatest losses are not due to absorption in the particle themselves but to scattering , which depends on relative values of the wavelength and the size of the particle. Thus the total path loss will be expressed as

$$Lp(d) = Lp(do) + 10n\log_{10}\left(\frac{d}{do}\right) + \alpha_{particle}{}^{d}[dB] - - - - - - - (2.20)$$

Where d_o = 0.99 distance of the reference far field from the transmitter $L_p(d_o)$ is free space path loss n is the propagation path loss exponent. For each type of scattering, the approximate relationship between the particle size and wavelength, and the wavelength power law of the attenuation coefficient is shown. From size parameter, Rayleigh scattering occurs when the atmospheric particle are mush smaller than the wavelength. Rayleigh scattering occurs primarily off of the gaseous molecules in the atmosphere. The attenuation coefficient varies at λ^{-4} (whereλ is the wavelength).

As the particle size approaches the wavelength, the scattering of radiation off the larger particles becomes more dominant in the forward direction as opposed to the backward direction. This type of scattering where the size parameter varies between 0.1 and 50, is call Mie scattering. For Mie scattering, the exponent in the power law dependence on wavelength for the attenuation coefficient varies from 1.6 to 0^{17}.

The third generalized scattering regime occurs when the atmospheric particles are much larger than the wavelength. For size parameters greater than 50, the scattering is called geometric or non –selective scattering. The scattering particle are large enough that the angular distribution of scattered radiation can be described by geometric optics. Rain drops, snow, hail, cloud droplets, and heavy fogs will geometrically scatter light. The scattering is called non-selective because there is no dependence of the attenuation coefficient on wavelength, i.e the power law wave length exponent is zero.

A more useful form of equation which depends only on the visibility, which is a much more commonly available parameter is:

$$\sigma = \frac{3.91}{v}\left(\frac{\lambda}{550nm}\right)^{-q} \quad \text{----------} \quad (2.21)$$

Where σ = atmospheric attenuation (or scattering) coefficient;

V= visibility (in km);

λ= wavelength (in nm); and

q = the size distribution of the scattering particles.

= 1.6 for high visibility (v>50km)

= 1.3 for average visibility (6km< V < 50kg)

$=0.585v^{1/3}$ for low visibility (V < 6km) .

This method of calculating the atmospheric attenuation coefficient is mostly preferred, because for a given wavelength, the amount of attenuation only depends on the visibility which is an easily obtainable parameter (either from airport or weather data).

The value of q is important because it determines the wavelength dependence of the attenuation coefficient and the physical type of scattering.

Equation (2.44) is referred in lasercom textbooks and used frequently in the lasercom literature. The function of q at low visibility .

2.6 ELECTRODYNAMICS

Considering that the harmattan particles serve as obstructions on the prorogation path and the fact that they are in complex motion, the effects of the induced energies or polarization may best be understood by a study on electrodynamics theory.

2.6.1 COULOMB'S LAW

Given two static charges q_1 and q_2, there is a force acting on each of them which is:

1. Proportional to the product of the magnitudes of the charges, being attractive for unlike charges and repulsive for like charges

2. Inversely proportional to the square of the distance between the charges.

3. Directed along the line between the charges.

In the form of an equation, the law states that

$$\overrightarrow{F_{21}} = k\frac{q_1 q_2}{\left|x_{2-} x_1\right|^2}\frac{x_2 - x_1}{\left|x_2 - x_1\right|} \text{----------(2.22)}$$

Where charge q_i is located at x_i, F_{21} is the force on charge 2 produced by charge 1, and k is a positive constant; vectors are denoted by boldface type.

In addition, the force satisfies a superposition law (or principle) in that the force F on a charge q in the presence of a number of other charges q_i at x_i, i = 1,...,n, is simply the sum of the forces arising from each of the latter as though it were the only other charge present . Thus,

$$F = kq\sum_{i=1}^{n}\frac{q\left(X - X_2\right)}{\left|X - X_i\right|} \text{----------(2.23)}$$

Given that q is at x

The constant k has units and magnitude which depend on the system of units employed.

2.6.2 Electric Field

It is customary and useful to introduce the concept of the electric field at the point X, which is written as E(x) and is defined as the force that would be experienced by a charge q at x, divided by q^3. Thus, for a distribution of charges q_i at x_i, i=1,2,…,n,

$$E(X) = \sum_{i=1}^{n} \frac{q_i}{4\pi\varepsilon r^2}$$ ----------(2.24)

The electric field has the property of being independent of the `test' charge q; it is a function of the charge distribution which gives rise to the force on the test charge, and, of course, of the test charge's position.

CHAPTER THREE

3.1 METHODOLOGY AND DATA COLLECTION

The records of monthly meteorological observations, obtained from the Meteorological Department of International Airport of N'Djamena (ASECNA) Chad, serves as the inputs to the foregoing analyses. The data covers the period from 2004 to 2006.

3.2 DATA COLLECTION

Measurement data were obtained from Meteorological Department of the International Airport of N'Djamena (ASECNA) Chad.

These data include: temperature, visibility, relative humidity, wind speed and wind direction, and are presented in Tables 3.1 to 3.13.

(a) Temperature

Table3.1 : Monthly Temperature for the Year 2004

Months / **Temp^{o}C**	**Janaruy**	**February**	**March**	**October**	**November**	**December**
Minimum	15.5	16.9	21.4	23.1	19.8	16.3
Average	23.6	25.7	29.4	30.0	28.2	24.7
Maximum	33.2	35.2	38.2	39.0	37.9	35.1

Table3.2 : Monthly Temperature for the Year 2005

Months / Temp°C	January	February	March	October	November	December
Minimum	14.7	21.8	25.4	22.2	19.5	17.3
Average	22.6	30.1	32.7	29.2	27.6	25.8
Maximum	31.8	39.8	41.3	36.5	37.6	36.2

Table3.3 : Monthly Temperature for the Year 2006

Months / Temp°C	January	February	March	October	November	December
Minimum	17.8	21.1	23.1	23.5	18.3	13.6
Average	26.3	29.4	31.1	29.3	26.2	22.5
Maximum	36.7	39.3	40.1	37.5	35.7	32.4

(b) Visibility

Table3.4 : Monthly Visibility for the Year 2004

visibility	January	February	March	October	November	December
Meters	600	600	300	800	1000	1000

Table3.5 : Monthly Visibility for the Year 2005

visibility	January	February	March	October	November	December
Meters	200	300	800	800	1000	1000

Table3.6 : Monthly Visibility for the Year 2006

visibility	January	February	March	October	November	December
Meters	1000	1000	300	600	1500	800

(c) Relative Humidity

Table3.7 : Monthly Record of Relative Humidity for the Year 2004

Months / Temp^{o}C	January	February	March	October	November	December
Minimum	26.2	25.8	19.1	58.4	29.8	28.5
Average	29.1	25.9	18.8	50.6	29.1	27.3
Maximum	20.4	20.2	16.1	50.1	28.1	27.1

Table3. 8 : Monthly Record of Relative Humidity for the Year 2005

Months / Temp^{o}C	January	February	March	October	November	December
Minimum	34.9	29.8	18.9	60.1	29.9	31.9
Average	24.6	22.5	18.2	55.2	29.5	31.7
Maximum	20.8	16.8	17.2	56.2	27.9	27.5

Table3.9 : Monthly Record of Relative Humidity for the Year 2006

Months / Temp°C	January	February	March	October	November	December
Minimum	35.1	26.2	19.2	59.9	33.5	35.9
Average	32.1	16.3	17.9	59.8	31.4	33.8
Maximum	16.8	16.9	15.9	59.4	28.1	30.8

(d) Dominant Wind

Table3.10 : Monthly Record of Dominant Wind for the Year 2004

visibility	January	February	March	October	November	December
Wind direction (degree)	360	40	40	40	40	40
Wind speed (m/s)	9	10	14	6	8	7

Table3.11 : Monthly Record of Dominant Wind for the Year 2005

visibility	January	February	March	October	November	December
Wind direction (degree)	40	40	40	180	20	360
Wind speed (m/s)	11	10	11	5	7	6

Table3.12 : Monthly Record of Dominant Wind for the Year 2006

Visibility	January	February	March	October	November	December
Wind direction (degree)	40	40	20	220	40	40
Wind speed (m/s)	7	8	8	6	8	8

(e) Table3.13 : Typical Atmospheric Scattering Particles Sizes [15]

Type	Radius(μm)	Size Parameter α	
Air Molecules		785nm	1550nm
Haze particle	0.0001	0.0008	0.0004
Fog droplet	0.01-1	0.08-8	0.04-4
Rain	1-20	8-160	4-80
Snow	100-10000	800-80000	400 - 40000
Hail	1000-5000	8000-40000	4000 -20000

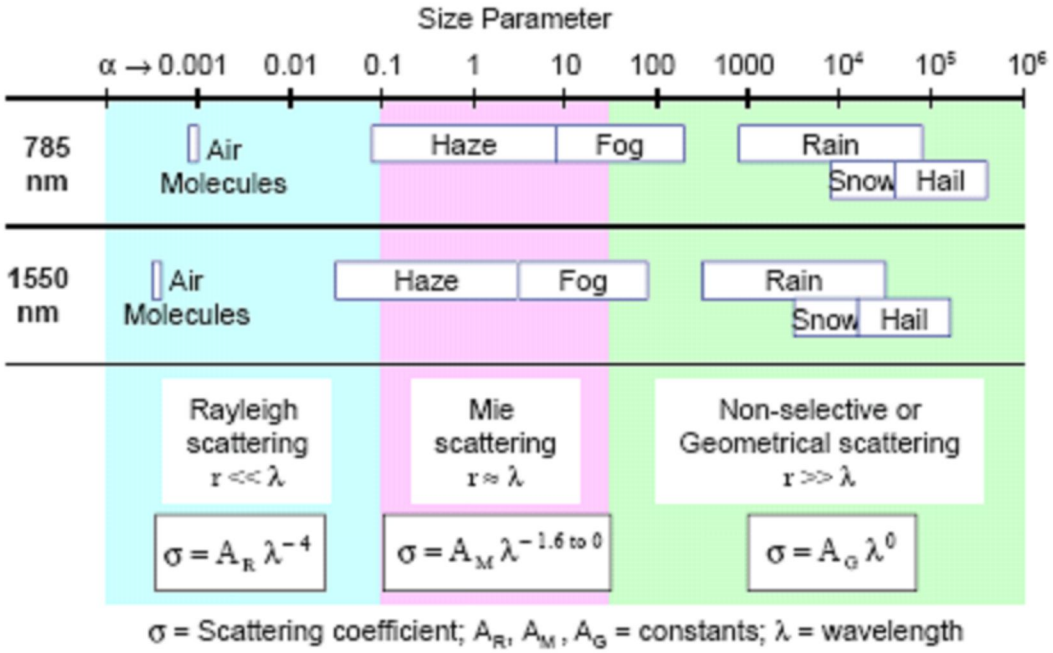

Fig 1:Particle Size Parameters [15]

Size parameters of atmospheric scattering particles in Table3.13 for Rayleigh, Mie and-selective or geometric scattering are also valuable resources in this work. For each type of scattering, the approximate relationship between the particle size and

wavelength and the wavelength power law of the attenuation coefficient are shown in Fig1

3.3 DISCUSION ON DATA.

The increases and decreases of the received signal strength at the various roads shows the effects of radio wave propagation impairments such as rooftop to street diffraction loss, multiscreen diffraction, shadowing, fading etc. These factors can be said to cause the drop in received signal strength at some distances of some roads. The received signal strength data collected may differ due to the fact that it was not taken directly, but send through contact with the radio frequency department of celtel Tchad.

3.4 MATHEMATICAL ANALYSIS

This offers quick results with a very good insight into what is actually happening with the process being evaluated, for example, it enables the relationship between the various parameters in the system to be seen. However, in most cases it is necessary to make many simplifying assumptions to enable such an analysis to be used. This is inevitably the case when communication is taking place over propagation channels with multipath and fading.

The effect of rain precipitation is usually expressed in terms of specific attenuation which is predicted with the aid of an empirical relationship given by [16]

$$\alpha_{rain} = a\rho^{b} dB/km \qquad \text{----------(3.1)}$$

Where ρ – the rainfall rate (mm/hr); a, b – regression coefficients which are a function of the frequency f, of the temperature T, of the drop size distribution and to a lesser extent, of the wave polarization.

The specific attenuation due to harmattan dust particle may be predicted using the specific particle attenuation variation (dB/m) given as:

$$\alpha_{particle}=a\,\rho_{.i}^{b} \quad \text{----------(3.2)}$$

Here the coefficients a and b are function of frequency f, of temperature T, and of the particle size distribution. The values of a and b for a given meteorological data are given by(3.3).

$$b = \frac{n\left(\sum_{i-1}^{n} x_i y_i\right) - \left(\sum_{i=1}^{n} xi\right)\left(\sum_{i=1}^{n} yi\right)}{n\left(\sum_{i=1}^{n} x_i^{\,2}\right) - \left(\sum_{i=1}^{n} x_i\right)^{2}} \quad \text{----------(3.3)}$$

$$a = \frac{\sum_{i=1}^{n} y_i - b\sum_{i=1}^{n} x_i}{n}$$

Where n – is the number of pairs of observation;

x – is the temperature of observations; and

y – particle size distributions.

The spatial harmattan particle density may be approximated by the empirical relationship given in equation (3.2).

$$\rho_i = \frac{(V_{fm} - V_i)\rho_p}{h} g/m^3 \text{ ----------(3.4)}$$

Where V_{fm}- the best visibility figure for the year (period) [m]

V_i – observed (measured) visibility profile[m]

ρ_p- mean particle density [g/m^3]

h- humidity profile (in decimals) [g/m^3]

The atmospheric attenuation impacted on microwave signals has been defined in equation (2.18)

$$\sigma = \frac{3.91}{v}\left(\frac{\lambda}{550nm}\right)^{-q} \text{ ---------- (3.5)}$$

Where σ = atmospheric attenuation (or scattering) coefficient;

V = visibility (in km);

λ = wavelength (in nm);

q = the size distribution of the scattering particles;

q = 1.6 for high visibility (v>50km);

q = 1.3 for average visibility (6km< V < 50kg);

$q = 0.585v^{1/3}$ for low visibility (V < 6km);

q = 1.3 for averaged visibility (6km <V< 50km);

q = 0.16V + 0.34 for haze visibility (1km < V< 6km);

q = V -0.5 for mist visibility (0.5km < V< 1km); and

q =0 for fog visibility (V < 0.5km).

CHAPTER FOUR

ANALYSIS AND RESULTS

4.0 INTRODUCTION

In this chapter, analysis of data obtained from the Meteorological Department of the International Airport of N'Djamena (ASECNA) Chad is carried out. Comparison is then made with computed values using the spatial harmattan particle density, the specific attenuation due to harmattan dust and the atmospheric loss model.

4.1 Results obtained using the spatial harmattan particle density model

Considering the empirical relation given by equation (3.4), harmattan dust density in air is:

$$\rho_i = \frac{(V_{fm} - V_i)\rho_p}{h} g/m^3 \text{ ----------(4.1)}$$

Substituting observed (measured) visibility profile, the best visibility figure period, mean particle density and humidity profile yields:

(a) for 2004

Vf_m=1550m ρ_p = 0.899

Month of January

Average temperature (^{0}C)

T(^{0}C) = 23.6

V_{fm} = 1550m

ρ_p = 0.899 g/m^3

V_i = 600m

h = 29.1 [g/m^3]

$$\rho_i = \frac{(1550 - 600_i)}{29.1} \times 0.899 g/m^3$$

$$\rho_i = 29.34 \text{g/m}^3$$

Minimum temperature (^{0}C)

T(^{0}C) = 15.5

h = 26.2

$$\rho_i = \frac{(1550 - 600_i)}{26.2} \times 0.899 g/m^3$$

$$\rho_i = 32.59 \text{ g/m}^3$$

Maximum temperature (^{0}C)

T(^{0}C) = 33.2

h = 20.4

$$\rho_i = \frac{(1550 - 600_i)}{20.4} \times 0.899 g/m^3$$

$$\rho_i = 41.86 \text{ g/m}^3$$

When the substitution was done for each month of the period of harmattan for 2004, the results are as presented in Tables 4.1 to 4.3:

Table 4.1: Harmattan dust density in air (ρ_i)

Jan 2004		**Feb 2004**		**March 2004**		**Oct 2004**		**Nov 2004**		**Dec 2004**	
T(^{0}C)	ρ_i(g/m^3)	T(^{0}C)	ρ_i(g/m^3)	T(^{0}C)	ρ_i(g/m^3)	T(^{0}C)	ρ_i(g/m^3)	T(^{0}C)	ρ_i(g/m^3)	T(^{0}C)	ρ_i(g/m^3)
15.5	32.59	16.9	33.10	21.4	58.83	23.1	11.54	19.8	16.59	16.3	17.34
23.6	29.34	25.7	32.97	29.4	59.77	30.0	13.32	28.2	16.99	24.7	18.11
33.2	41.86	35.2	35.2	38.2	69.79	39.0	13.45	37.9	17.59	35.1	18.24

(b) For 2005

Vf_m=1550m ρ_p = 0.899 g/m^3

Month of January

Minimum Temperature (^{0}C)

T(^{0}C) = 14.7

h = 34.9

$$\rho_i = \frac{(1550 - 200_i)}{34.9} \times 0.899 g/m^3$$

$$\rho_i = 34.77 \text{ g/m}^3$$

Average Temperature (^{0}C)

T(^{0}C) = 22.6

h = 24.6

$$\rho_i = \frac{(1550 - 200_i)}{24.6} \times 0.899 g/m^3$$

$$\rho_i = 49.33 \text{g/m}^3$$

Maximum temperature (^{0}C)

T(^{0}C) = 31.8

h = 20.8

$$\rho_i = \frac{(1550 - 200_i)}{20.8} \times 0.899 g/m^3$$

$$\rho_i = 58.34 \text{ g/m}^3$$

Table 4.2: Harmattan dust density in air (ρ_i)

Jan 2005		**Feb 2005**		**March 2005**		**Oct 2005**		**Nov 2005**		**Dec 2005**	
T(^{0}C)	ρ_i(g/m^3)	T(^{0}C)	ρ_i(g/m^3)	T(^{0}C)	ρ_i(g/m^3)	T(^{0}C)	ρ_i(g/m^3)	T(^{0}C)	ρ_i(g/m^3)	T(^{0}C)	ρ_i(g/m^3)
14.7	34.77	21.8	37.70	25.4	35.67	22.2	11.21	19.5	16.53	17.3	15.50
22.6	49.33	30.1	49.94	32.7	37.04	29.2	12.21	27.6	16.76	25.8	15.59
31.8	58.34	39.8	66.88	41.3	39.20	36.5	11.99	37.6	17.72	36.2	17.98

(c) For 2006

Vf_m=1550m ρ_p = 0.899 g/m^3

Month of January

Minimum Temperature (^{0}C)

T(^{0}C) = 17.8

h = 35.1

$$\rho_i = \frac{(1550 - 1000_i)}{35.1} \times 0.899 g/m^3$$

$$\rho_i = 14.08 \text{ g/m}^3$$

Average Temperature (^{0}C)

T(^{0}C) = 26.3

h = 32.1

$$\rho_i = \frac{(1550 - 1000_i)}{32.1} \times 0.899 g/m^3$$

$$\rho_i = 15.40 \text{g/m}^3$$

Maximum temperature (^{0}C)

T(^{0}C) = 36.7

h = 16.8

$$\rho_i = \frac{(1550 - 1000_i)}{16.8} \times 0.899 g/m^3$$

$$\rho_i = 29.43 \text{ g/m}^3$$

Table 4.3: Harmattan dust density in air (ρ_i)

Jan 2006		**Feb 2006**		**March 2006**		**Oct 2006**		**Nov 2006**		**Dec 2006**	
T(^{0}C)	ρ_i(g/m^3)	T(^{0}C)	ρ_i(g/m^3)	T(^{0}C)	ρ_i(g/m^3)	T(^{0}C)	ρ_i(g/m^3)	T(^{0}C)	ρ_i(g/m^3)	T(^{0}C)	ρ_i(g/m^3)
17.8	14.08	21.1	18.87	23.1	58.52	23.5	14.25	18.3	1.34	13.6	18.78
26.3	15.40	29.4	30.33	31.1	62.77	29.3	14.28	26.2	1.43	22.5	19.94
36.7	29.43	39.3	29.25	40.1	70.67	37.5	14.37	35.7	1.59	32.4	21.89

4.2 RESULTS OBTAINED USING THE SPECIFIC ATTENUATION DUE TO HARMATTAN DUST PARTICLES

From equation (3.3) regression coefficients which are function of the frequency f, of the temperature T, of the size parameter and to a lesser extent, of the wave polarization (a, b) can be determined as follows:

$$b = \frac{n\left(\sum_{i=1}^{n} X_i Y_i\right) - \left(\sum_{i=1}^{n} X_i\right)\left(\sum_{i=1}^{n} Y_i\right)}{\left(\sum_{i=1}^{n} X_i^2\right) - \left(\sum_{i=1}^{n} X_i\right)^2} \text{ ----------(4.2)}$$

$$a = \frac{\sum_{i=1}^{n} y_i - b\sum_{i=1}^{n} x_i}{n}$$

y_{i1}= particle size distribution

n_i = is the number of months of observations which is 6

x_i= is the temperature of observations

Substituting for n_1 x_i ,and y_i we have:

With reference to Table 3.13 in page 27, it can thus be assumed that the size parameters have the following distribution.

y_1= 0.001	y_2 = 0.01	y_3= 0.1	y_4 = 1	y_5 = 10	y_6 = 100
y_1= 0.01	y_2 = 0.1	y_3 = 1	y_4 = 10	y_5 = 100	y_6 = 0.001
y_1= 0. 1	y_2 = 1	y_3 = 10	y_4 = 100	y_5 = 0.001	y_6 = 0.01
y_1= 1	y_2 =10	y_3 = 100	y_4 = 0.001	y_5 = 0.01	y_6 = 0.1
y_1= 10	y_2 =100	y_3 = 0.001	y_4 = 0.01	y_5 = 0.1	y_6 = 1
y_1= 100	y_2 = 0.001	y_3 = 0.01	y_4 = 0.1	y_5 = 1	y_6 = 10n = 6

n corresponds to number of months over the period.

(a)For 2004

$$6(x_1y_1 + x_2y_2 + x_3y_3 + x_4y_4 + x_5y_5 + x_6y_6)$$

$$6(23.6 \times 0.001 + 25.7 \times 0.01 + 29.4 \times 0.1 + 30.0 \times 1 + 28.2 \times 10 + 24.7 \times 100)$$

$$6\left(\sum_{i=1}^{6} x_i y_i\right) = 16711.32$$

$$(x_1 + x_2 + x_3 + x_4 + x_5 + x_6)$$

$$23.6 + 25.7 + 29.4 + 30.0 + 28.2 + 24.7$$

$$\left(\sum_{i=1}^{6} y_i\right) = 111.11$$

$$6(x_1^2 + x_2^2 + x_3^2 + x_4^2 + x_5^2 + x_6^2)$$

$$6\left[(23.6)^2 + (25.7)^2 + (29.4)^2 + (30.0)^2 + (28.2)^2 + (24.7)^2\right]$$

$$6\left(\sum_{i=1}^{6} x_i^2\right) = 26322.84$$

$$(x_1 + x_2 + x_3 + x_4 + x_5 + x_6)^2$$

$$(23.6 + 257 + 29.4 + 30.0 + 28.2 + 24.7)^2$$

$$\left(\sum_{i=1}^{6} x_i\right)^2 = 26114.56$$

$$b = \frac{16711.32 - (161.6 \times 111.11)}{26322.84 - 26114.56}$$

$$b = -5.97$$

$$a = \frac{111.11 + (5.97 \times 161.6)}{6}$$

$$a = 179.31$$

By following the process all values of a and b can be determined for each year. The results are presented in Tables 4.4 – 4.12.

Table 4.4: Minimum Temperature for 2004

Size parameter	β	a	b
Air molecules	0.001	114.19	-5.08
	0.01	-37.98	3
	0.1	-150.98	9
Haze	1	-75.08	4.97
	10	110.23	-4.87
Fog	100	161.65	-7.60

Table 4.5: Average Temperature for 2004

Size parameter	β	a	b
Air molecules	0.001	179.31	-5.97
	0.01	-105.1	4.59
	0.1	-237.07	9.49
Haze	1	-160.31	6.64
	10	141.6	-4.57
Fog	100	457.80	-16.31

Table 4.6: Maximum Temperature for 2004

Size parameter	β	a	b
Air molecules	0.001	183.19	-4.52
	0.01	-228.86	6.79
	0.1	-369.49	10.65
Haze	1	-210.28	6.28
	10	241.49	-6.12
Fog	100	494.70	-13.07

(b) For 2005

Table 4.7: Minimum Temperature for 2005

Size parameter	β	a	b
Air molecules	0.001	98.51	-3.97
	0.01	29.19	-0.53
	0.1	-53.01	3.55
Haze	1	-129.78	7.36
	10	-11.10	1.47
Fog	100	177.30	-7.88

Table 4.8: Average Temperature for 2005

Size parameter	β	a	b
Air molecules	0.001	118.47	-3.57
	0.01	28.87	-0.37
	0.1	-57.36	2.71
Haze	1	-200.16	7.81
	10	-50.64	2.47
Fog	100	271.9	-9.05

Table 4.9: Maximum Temperature for 2005

Size parameter	β	a	b
Air molecules	0.001	83.99	-1.76
	0.01	-6.77	0.68
	0.1	36.74	-0.49
Haze	1	-275.73	7.91
	10	-121.72	3.77
Fog	100	394.23	-10.10

c) For 2006

Table 4.10: Minimum Temperature for 2006

Size parameter	β	a	b
Air molecules	0.001	186	-8.56
	0.01	41.60	-1.18
	0.1	-682.16	35.81
Haze	1	-82.83	5.18
	10	-17.28	1.83
Fog	100	84.06	-3.35

Table 4.11: Average Temperature for 2006

Size parameter	β	a	b
Air molecules	0.001	314.60	-10.78
	0.01	78.39	-2.18
	0.1	-108.10	4.61
Haze	1	-199.56	7.94
	10	-82.55	3.68
Fog	100	114.37	-3.49

Table 4.12: Maximum Temperature for 2006

Size parameter	β	a	b
Air molecules	0.001	471.15	-12.25
	0.01	130.84	-3.04
	0.1	-67.57	2.33
Haze	1	-309.22	8.87
	10	-202.44	5.98
Fog	100	87.98	-1.88

(d) The specific particle attenuation variation (dB/m) is given as:

$\alpha_{particle}$=a $\rho_{.i}^{b}$

For 2004

Minimum Temperature (2004)

The Specific particle attenuation variation for the Month of January is calculated as follows:

$$\rho_i(g/m^3) = 32.59$$

$$\alpha_{particle} = 114.19 \times 32.59(-5.08) = 2.35 \times 10^{-6}$$

$$\alpha_{particle} = -37.98 \times 32.59(3) = -1.31 \times 10^{6}$$

$$\alpha_{particle} = -150.98 \times 32.59(9) = -6.26 \times 10^{15}$$

$$\alpha_{particle} = -75.08 \times 32.59(4.97) = -2.48 \times 10^{9}$$

$$\alpha_{particle} = 110.23 \times 32.59(-4.87) = 4.71 \times 10^{-6}$$

$$\alpha_{particle} = 161.65 \times 32.59(-7.60) = 511.84 \times 10^{-12}$$

By following the same process, the specific particle attenuation variation of each year are determined and presented in Tables 4.13 – 4.66.

Table 4.13: The Specific particle attenuation variation for Month of January 2004

Size parameter	β	a	b	ρ_i (g/m^3)	α(dB/m)
Air molecules	0.001	114.19	-5.08	32.59	2.35 x 10^{-6}
	0.01	-37.98	3	32.59	-1.3 x 10^{6}
	0.1	-150.98	9	32.59	-6.26 x 10^{15}
Haze	1	-75.08	4.97	32.59	-2.48 x 10^{9}
	10	110.23	-4.87	32.59	4.71 x 10^{-6}
Fog	100	161.65	-7.60	32.59	511.84 x 10^{-12}

Table 4.14:The Specific particle attenuation variation for Month of February 2004

Size parameter	β	a	b	ρ_i (g/m^3)	α(dB/m)
Air molecules	0.001	114.19	-5.08	33.10	2.17×10^{-6}
	0.01	-37.98	3	33.10	-1.37×10^{6}
	0.1	-150.98	9	33.10	-7.20×10^{15}
Haze	1	-75.08	4.97	33.10	-2.68×10^{9}
	10	110.23	-4.87	33.10	3.08×10^{-6}
Fog	100	161.65	-7.60	33.10	454.86×10^{-12}

Table 4.15: The Specific particle attenuation variation for Month of March 2004

Size parameter	β	a	b	ρ_i (g/m^3)	α(dB/m)
Air molecules	0.001	114.19	-5.08	58.83	1.16×10^{-7}
	0.01	-37.98	3	58.83	-7.73×10^{6}
	0.1	-150.98	9	58.83	-1.27×10^{18}
Haze	1	-75.08	4.97	58.83	-4.68×10^{10}
	10	110.23	-4.87	58.83	2.65×10^{-7}
Fog	100	161.65	-7.60	58.83	5.74×10^{-12}

Table 4.16: The Specific particle attenuation variation for Month of October 2004

Size parameter	β	a	b	ρ_i (g/m^3)	α(dB/m)
Air molecules	0.001	114.19	-5.08	11.54	4.58×10^{-4}
	0.01	-37.98	3	11.54	-58.36×10^{3}
	0.1	-150.98	9	11.54	-5.47×10^{11}
Haze	1	-75.08	4.97	11.54	-14.27×10^{6}
	10	110.23	-4.87	11.54	740.21×10^{-6}
Fog	100	161.65	-7.60	11.54	1.36×10^{-6}

Table 4.17: The Specific particle attenuation variation for Month of November 2004

Size parameter	β	a	b	ρ_i (g/m^3)	α(dB/m)
Air molecules	0.001	114.19	-5.08	16.59	72.57×10^{-6}
	0.01	-37.98	3	16.59	-173.41×10^{3}
	0.1	-150.98	9	16.59	-14.37×10^{12}
Haze	1	-75.08	4.97	16.59	-86.72×10^{6}
	10	110.23	-4.87	16.59	126.37×10^{-6}
Fog	100	161.65	-7.60	16.59	8.664×10^{-8}

Table 4.18: The Specific particle attenuation variation for Month of December 2004

Size parameter	β	a	b	ρ_i (g/m^3)	α(dB/m)
Air molecules	0.001	114.19	-5.08	17.34	57.97×10^{-6}
	0.01	-37.98	3	17.34	-198.01×10^{3}
	0.1	-150.98	9	17.34	-21.39×10^{12}
Haze	1	-75.08	4.97	17.34	-108.04×10^{6}
	10	110.23	-4.87	17.34	101.88×10^{-6}
Fog	100	161.65	-7.60	17.34	6.191×10^{-8}

(e) The Specific particle attenuation variation for Average Temperature 2004

Table 4.19: The Specific particle attenuation variation for Month of January 2004

Size parameter	β	a	b	ρ_i (g/m^3)	α(dB/m)
Air molecules	0.001	179.31	-5.97	29.34	3.11×10^{-7}
	0.01	-105.1	4.59	29.34	-571.80×10^{6}
	0.1	-237.07	9.49	29.34	-2.00×10^{6}
Haze	1	-160.31	6.64	29.34	-8.88×10^{11}
	10	141.6	-4.57	29.34	2.78×10^{-5}
Fog	100	457.80	-16.31	29.34	5.32×10^{-22}

Table 4.20: The Specific particle attenuation variation for Month of February 2004

Size parameter	β	a	b	ρ_i (g/m^3)	α(dB/m)
Air molecules	0.001	179.31	-5.97	32.97	1.55×10^{-7}
	0.01	-105.1	4.59	32.97	-976.71×10^{6}
	0.1	-237.07	9.49	32.97	-6.05×10^{16}
Haze	1	-160.31	6.64	32.97	-1.92×10^{12}
	10	141.6	-4.57	32.97	1.63×10^{-5}
Fog	100	457.80	-16.31	32.97	7.94×10^{-23}

Table 4.21: Specific particle attenuation variation for Month of March 2004

Size parameter	β	a	b	ρ_i (g/m^3)	α(dB/m)
Air molecules	0.001	179.31	-5.97	59.77	4.22×10^{-9}
	0.01	-105.1	4.59	59.77	-1.49×10^{10}
	0.1	-237.07	9.49	59.77	-1.71×10^{19}
Haze	1	-160.31	6.64	59.77	-1.00×10^{14}
	10	141.6	-4.57	59.77	1.07×10^{-6}
Fog	100	457.80	-16.31	59.77	4.85×10^{-27}

Table 4.22: The Specific particle attenuation variation for Month of October 2004

Size parameter	β	a	b	ρ_i (g/m^3)	α(dB/m)
Air molecules	0.001	179.31	-5.97	13.32	3.46×10^{-5}
	0.01	-105.1	4.59	13.32	-15.24×10^{6}
	0.1	-237.07	9.49	13.32	-1.11×10^{13}
Haze	1	-160.31	6.64	13.32	-469×10^{9}
	10	141.6	-4.57	13.32	1.02×10^{-3}
Fog	100	457.80	-16.31	13.32	2.08×10^{-16}

Table 4.23: The Specific particle attenuation variation for Month of November 2004

Size parameter	β	a	b	ρ_i (g/m^3)	α(dB/m)
Air molecules	0.001	179.31	-5.97	16.99	8.11×10^{-6}
	0.01	-105.1	4.59	16.99	46.57×10^{6}
	0.1	-237.07	9.49	16.99	-112.04×10^{12}
Haze	1	-160.31	6.64	16.99	-23.62×10^{9}
	10	141.6	-4.57	16.99	338.12×10^{-6}
Fog	100	457.80	-16.31	16.99	3.94×10^{-18}

Table 4.24: The Specific particle attenuation variation for Month of December 2004

Size parameter	β	a	b	ρ_i (g/m^3)	α(dB/m)
Air molecules	0.001	179.31	-5.97	18.11	5.54×10^{-6}
	0.01	-105.1	4.59	18.11	-62.43×10^{6}
	0.1	-237.07	9.49	18.11	-205.36×10^{12}
Haze	1	-160.31	6.64	18.11	-36.10×10^{9}
	10	141.6	-4.57	18.11	252.56×10^{-6}
Fog	100	457.80	-16.31	18.11	1.39×10^{-18}

f)The Specific particle attenuation variation for Maximum Temperature 2004

Table 4.25: The Specific particle attenuation variation for Month of January 2004

Size parameter	β	a	b	ρ_i (g/m^3)	α(dB/m)
Air molecules	0.001	183.19	-4.52	41.86	8.55×10^{-6}
	0.01	-228.86	6.79	41.86	-2.35×10^{3}
	0.1	-369.49	10.65	41.86	-6.91×10^{19}
Haze	1	-210.28	6.28	41.86	-3.21×10^{12}
	10	241.49	-6.12	41.86	2.86×10^{-8}
Fog	100	494.70	-13.07	41.86	3.14×10^{-19}

Table 4.26: The specific particle attenuation variation for Month of February 2004

Size parameter	β	a	b	ρ_i (g/m^3)	α(dB/m)
Air molecules	0.001	183.19	-4.52	42.27	8.18×10^{-6}
	0.01	-228.86	6.79	42.27	-2.51×10^{13}
	0.1	-369.49	10.65	42.27	-7.67×10^{19}
Haze	1	-210.28	6.28	42.27	-3.64×10^{12}
	10	241.49	-6.12	42.27	2.70×10^{-8}
Fog	100	494.70	-13.07	42.27	2.76×10^{-19}

Table 4.27: The specific particle attenuation variation for Month of March 2004

Size parameter	β	a	b	ρ_i (g/m^3)	α(dB/m)
Air molecules	0.001	183.19	-4.52	69.79	8.49×10^{-7}
	0.01	-228.86	6.79	69.79	-7.56×10^{14}
	0.1	-369.49	10.65	69.79	-1.59×10^{22}
Haze	1	-210.28	6.28	69.79	-7.97×10^{13}
	10	241.49	-6.12	69.79	1.25×10^{-9}
Fog	100	494.70	-13.07	69.79	3.94×10^{-22}

Table 4.28:The specific particle attenuation variation for Month of October 2004

Size parameter	β	a	b	ρ_i (g/m^3)	α(dB/m)
Air molecules	0.001	183.19	-4.52	13.45	1.44×10^{-3}
	0.01	-228.86	6.79	13.45	-1.05×10^{10}
	0.1	-369.49	10.65	13.45	-3.87×10^{14}
Haze	1	-210.28	6.28	13.45	-2.57×10^{9}
	10	241.49	-6.12	13.45	2.98×10^{-5}
Fog	100	494.70	-13.07	13.45	8.74×10^{-13}

Table 4.29: The specific particle attenuation variation for Month of November 2004

Size parameter	β	a	b	ρ_i (g/m^3)	α(dB/m)
Air molecules	0.001	183.19	-4.52	17.59	4.30×10^{-4}
	0.01	-228.86	6.79	17.59	-6.53×10^{10}
	0.1	-369.49	10.65	17.59	-6.75×10^{15}
Haze	1	-210.28	6.28	17.59	-1.39×10^{10}
	10	241.49	-6.12	17.59	5.78×10^{-6}
Fog	100	494.70	-13.07	17.59	2.62×10^{-14}

Table 4.30: The specific particle attenuation variation for Month of December 2004

Size parameter	β	a	b	ρ_i (g/m^3)	α(dB/m)
Air molecules	0.001	183.19	-4.52	18.24	3.65×10^{-4}
	0.01	-228.86	6.79	18.24	-8.35×10^{8}
	0.1	-369.49	10.65	18.24	-9.94×10^{15}
Haze	1	-210.28	6.28	18.24	-1.74×10^{10}
	10	241.49	-6.12	18.24	4.6×10^{-6}
Fog	100	494.70	-13.07	18.24	1.63×10^{-14}

(g)The specific particle attenuation variation for Minimum Temperature 2005

Table 4.31: The Specific particle attenuation variation for month of January 2005

Size parameter	β	a	b	ρ_i (g/m^3)	α(dB/m)
Air molecules	0.001	98.51	-3.97	34.77	74.97×10^{-6}
	0.01	29.19	-0.53	34.77	4.45
	0.1	-53.01	3.55	34.77	-15.69×10^{6}
Haze	1	-129.78	7.36	34.77	-28.60×10^{12}
	10	-11.10	1.47	34.77	-2.04×10^{3}
Fog	100	177.30	-7.88	34.77	127.06×10^{-12}

Table 4.32: The Specific particle attenuation for Month of February 2005

Size parameter	β	a	b	ρ_i (g/m^3)	α(dB/m)
Air molecules	0.001	98.51	-3.97	37.70	54.37 x 10^{-6}
	0.01	29.19	-0.53	37.70	4.26
	0.1	-53.01	3.55	37.70	-20.91 x 10^{6}
Haze	1	-129.78	7.36	37.70	-51.88 x 10^{12}
	10	-11.10	1.47	37.70	-2.30 x 10^{3}
Fog	100	177.30	-7.88	37.70	67.16 x 10^{-12}

Table 4.33: The Specific particle attenuation for Month of March 2005

Size parameter	β	a	b	ρ_i (g/m^3)	α(dB/m)
Air molecules	0.001	98.51	-3.97	35.67	67.73 x 10^{-6}
	0.01	29.19	-0.53	35.67	4.39
	0.1	-53.01	3.55	35.67	-17.18 x 10^{6}
Haze	1	-129.78	7.36	35.67	-34.52 x 10^{12}
	10	-11.10	1.47	35.67	-2.12 x 10^{3}
Fog	100	177.30	-7.88	35.67	103.88 x 10^{-12}

Table 4.34: The Specific particle attenuation for Month of October 2005

Size parameter	β	a	b	ρ_i (g/m^3)	α(dB/m)
Air molecules	0.001	98.51	-3.97	11.21	6.70×10^{-3}
	0.01	29.19	-0.53	11.21	8.10
	0.1	-53.01	3.55	11.21	-282.13×10^{3}
Haze	1	-129.78	7.36	11.21	-6.89×10^{9}
	10	-11.10	1.47	11.21	-387.47
Fog	100	177.30	-7.88	11.21	950.20×10^{-9}

Table 4.35: The Specific particle attenuation for Month of November 2005

Size parameter	β	a	b	ρ_i (g/m^3)	α(dB/m)
Air molecules	0.001	98.51	-3.97	16.53	1.43×10^{-3}
	0.01	29.19	-0.53	16.53	6.60
	0.1	-53.01	3.55	16.53	-1.12×10^{6}
Haze	1	-129.78	7.36	16.53	-120.14×10^{9}
	10	-11.10	1.47	16.53	-685.77
Fog	100	177.30	-7.88	16.53	44.53×10^{-9}

Table 4.36: The Specific particle attenuation for Month of December 2005

Size parameter	β	a	b	ρ_i (g/m^3)	α(dB/m)
Air molecules	0.001	98.51	-3.97	15.5	1.85×10^{-3}
	0.01	29.19	-0.53	15.5	6.82
	0.1	-53.01	3.55	15.5	-891.32×10^{3}
Haze	1	-129.78	7.36	15.5	-74.82×10^{9}
	10	-11.10	1.47	15.5	-623.89
Fog	100	177.30	-7.88	15.5	73.94×10^{-9}

(h) The Specific particle attenuation for Average Temperature 2005

Table 4.37: The Specific particle attenuation variation for Month of January 2005.

Size parameter	β	a	b	ρ_i (g/m^3)	α(dB/m)
Air molecules	0.001	118.47	-3.57	49.33	1.06×10^{-4}
	0.01	28.87	-0.37	49.33	6.82
	0.1	-57.36	2.71	49.33	-2.22×10^{6}
Haze	1	-200.16	7.81	49.33	-3.34×10^{15}
	10	-50.64	2.47	49.33	-769.97×10^{3}
Fog	100	271.9	-9.05	49.33	129.34×10^{-15}

Table 4.38: The Specific particle attenuation variation for Month of February 2005

Size parameter	β	a	b	ρ_i (g/m^3)	α(dB/m)
Air molecules	0.001	118.47	-3.57	49.94	1.02×10^{-6}
	0.01	28.87	-0.37	49.94	6.79
	0.1	-57.36	2.71	49.94	-2.29×10^{6}
Haze	1	-200.16	7.81	49.94	-3.68×10^{15}
	10	-50.64	2.47	49.94	-793.70×10^{3}
Fog	100	271.9	-9.05	49.94	129.34×10^{-15}

Table 39: The Specific particle attenuation variation for Month of March 2005

Size parameter	β	a	b	ρ_i (g/m^3)	α(dB/m)
Air molecules	0.001	118.47	-3.57	37.04	297.47×10^{-6}
	0.01	28.87	-0.37	37.04	7.58
	0.1	-57.36	2.71	37.04	-1.02×10^{6}
Haze	1	-200.16	7.81	37.04	-357.02×10^{12}
	10	-50.64	2.47	37.04	-379.41×10^{3}
Fog	100	271.9	-9.05	37.04	1.72×10^{-12}

Table 4.40: The Specific particle attenuation variation for Month of October 2005 .

Size parameter	β	a	b	ρ_i (g/m^3)	α(dB/m)
Air molecules	0.001	118.47	-3.57	12.21	15.63 x 10^{-3}
	0.01	28.87	-0.37	12.21	11.43
	0.1	-57.36	2.71	12.21	-50.53 x 10^{3}
Haze	1	-200.16	7.81	12.21	-51.46 x 10^{9}
	10	-50.64	2.47	12.21	-24.47 x 10^{3}
Fog	100	271.9	-9.05	12.21	39.77 x 10^{-9}

Table 4.41: The Specific particle attenuation variation for Month of November 2005

Size parameter	β	a	b	ρ_i (g/m^3)	α(dB/m)
Air molecules	0.001	118.47	-3.57	16.76	5.10 x 10^{-3}
	0.01	28.87	-0.37	16.76	10.18
	0.1	-57.36	2.71	16.76	-118.27 x 10^{3}
Haze	1	-200.16	7.81	16.76	-712.56 x 10^{9}
	10	-50.64	2.47	16.76	-53.11 x 10^{3}
Fog	100	271.9	-9.05	16.76	2.32 x 10^{-9}

Table 4.42: The Specific particle attenuation variation for Month of December 2005

Size parameter	β	a	b	ρ_i (g/m^3)	α(dB/m)
Air molecules	0.001	118.47	-3.57	15.59	6.53 x 10^{-3}
	0.01	28.87	-0.37	15.59	10.44
	0.1	-57.36	2.71	15.59	-97.99 x 10^{3}
Haze	1	-200.16	7.81	15.59	-414.48 x 10^{9}
	10	-50.64	2.47	15.59	-44.75 x 10^{3}
Fog	100	271.9	-9.05	15.59	4.35 x 10^{-9}

(i) The Specific particle attenuation variation for Maximum Temperature 2005

Table 4.43 The Specific particle attenuation variation for Month of January 2005

Size parameter	β	a	b	ρ_i (g/m^3)	α(dB/m)
Air molecules	0.001	83.99	-1.76	58.34	65.48 x 10^{-3}
	0.01	-6.77	0.68	58.34	-107.50
	0.1	36.74	-0.49	58.34	5.00
Haze	1	-275.73	7.91	58.34	-25.66 x 10^{15}
	10	-121.72	3.77	58.34	-553.42 x 10^{6}
Fog	100	394.23	-10.10	58.34	574.76 x 10^{-18}

Table 4.44: The Specific particle attenuation variation for Month of February 2005

Size parameter	β	a	b	ρ_i (g/m^3)	α(dB/m)
Air molecules	0.001	83.99	-1.76	66.88	51.48 x 10^{-3}
	0.01	-6.77	0.68	66.88	-117.97
	0.1	36.74	-0.49	66.88	4.68
Haze	1	-275.73	7.91	66.88	-75.60 x 10^{15}
	10	-121.72	3.77	66.88	-926.25 x 10^{6}
Fog	100	394.23	-10.10	66.88	144.62 x 10^{-18}

Table 4.45: The Specific particle attenuation variation for Month of March 2005

Size parameter	β	a	b	ρ_i (g/m^3)	α(dB/m)
Air molecules	0.001	83.99	-1.76	39.20	131.83 x 10^{-3}
	0.01	-6.77	0.68	39.20	-82.03
	0.1	36.74	-0.49	39.20	6.08
Haze	1	-275.73	7.91	39.20	-1.10 x 10^{15}
	10	-121.72	3.77	39.20	-123.6 x 10^{6}
Fog	100	394.23	-10.10	39.20	31.88 x 10^{-15}

Table 4.46: The Specific particle attenuation variation for Month of October 2005

Size parameter	β	a	b	ρ_i (g/m^3)	α(dB/m)
Air molecules	0.001	83.99	-1.76	11.99	1.06
	0.01	-6.77	0.68	11.99	-36.65
	0.1	36.74	-0.49	11.99	10.87
Haze	1	-275.73	7.91	11.99	-94.17×10^{9}
	10	-121.72	3.77	11.99	-1.42×10^{6}
Fog	100	394.23	-10.10	11.99	5.00×10^{-9}

Table 4.47: The Specific particle attenuation variation for Month of November 2005

Size parameter	β	a	b	ρ_i (g/m^3)	α(dB/m)
Air molecules	0.001	83.99	-1.76	17.72	533.25×10^{-3}
	0.01	-6.77	0.68	17.72	-47.81
	0.1	36.74	-0.49	17.72	8.98
Haze	1	-275.73	7.91	17.72	-2.06×10^{12}
	10	-121.72	3.77	17.72	-6.19×10^{6}
Fog	100	394.23	-10.10	17.72	96.88×10^{-12}

Table 4.48: The Specific particle attenuation variation for Month of December 2005

Size parameter	β	a	b	ρ_i (g/m^3)	α(dB/m)
Air molecules	0.001	83.99	-1.76	17.98	519.75 x 10^{-3}
	0.01	-6.77	0.68	17.98	-48.28
	0.1	36.74	-0.49	17.98	8.91
Haze	1	-275.73	7.91	17.98	-2.32 x 10^{12}
	10	-121.72	3.77	17.98	-6.54 x 10^{6}
Fog	100	394.23	-10.10	17.98	83.63 x 10^{-12}

(J) The Specific particle attenuation variation For Minimum Temperature (2006)

Table 4.49: The Specific Particle attenuation variation for month of January 2006

Size parameter	β	a	b	ρ_i (g/m^3)	α(dB/m)
Air molecules	0.001	186	-8.56	14.08	27.38 x 10^{-9}
	0.01	41.60	-1.18	14.08	1.83
	0.1	-682.16	35.81	14.08	-92.33 x 10^{42}
Haze	1	-82.83	5.18	14.08	-73.78 x 10^{6}
	10	-17.28	1.83	14.08	-2.24 x 10^{3}
Fog	100	84.06	-3.35	14.08	11.93 x 10^{-3}

Table 4.50: The Specific particle attenuation variation for Month of February 2006

Size parameter	β	a	b	ρ_i (g/m^3)	α(dB/m)
Air molecules	0.001	186	-8.56	18.87	2.23×10^{-9}
	0.01	41.60	-1.18	18.87	1.29
	0.1	-682.16	35.81	18.87	-3.30×10^{48}
Haze	1	-82.83	5.18	18.87	-336.26×10^{6}
	10	-17.28	1.83	18.87	-3.73×10^{3}
Fog	100	84.06	-3.35	18.87	4.47×10^{-3}

Table 4.51: The Specific particle attenuation variation for Month of March 2006

Size parameter	β	a	b	ρ_i (g/m^3)	α(dB/m)
Air molecules	0.001	186	-8.56	58.52	138.48×10^{-15}
	0.01	41.60	-1.18	58.52	341.72×10^{-3}
	0.1	-682.16	35.81	58.52	-1.32×10^{66}
Haze	1	-82.83	5.18	58.52	-118.25×10^{9}
	10	-17.28	1.83	58.52	-24.67×10^{9}
Fog	100	84.06	-3.35	58.52	100.95×10^{-6}

Table 4.52: The Specific particle attenuation variation for Month of October 2006

Size parameter	β	a	b	ρ_i (g/m^3)	α(dB/m)
Air molecules	0.001	186	-8.56	14.25	24.70×10^{-9}
	0.01	41.60	-1.18	14.25	1.8
	0.1	-682.16	35.81	14.25	-141.9×10^{42}
Haze	1	-82.83	5.18	14.25	-78.51×10^{6}
	10	-17.28	1.83	14.25	-2.3×10^{3}
Fog	100	84.06	-3.35	14.25	11.46×10^{-3}

Table 4.53: The Specific particle attenuation variation for Month of October 2006

Size parameter	β	a	b	ρ_i (g/m^3)	α(dB/m)
Air molecules	0.001	186	-8.56	1.34	15.18
	0.01	41.60	-1.18	1.34	29.45
	0.1	-682.16	35.81	1.34	-24.29×10^{6}
Haze	1	-82.83	5.18	1.34	-377.21
	10	-17.28	1.83	1.34	-29.52
Fog	100	84.06	-3.35	1.34	31.53

Table 4.54: The Specific particle attenuation variation for Month of November 2006

Size parameter	β	a	b	ρ_i (g/m^3)	α(dB/m)
Air molecules	0.001	186	-8.56	18.78	2.32×10^{-9}
	0.01	41.60	-1.18	18.78	1.3
	0.1	-682.16	35.81	18.78	-2.78×10^{42}
Haze	1	-82.83	5.18	18.78	-328.04×10^{6}
	10	-17.28	1.83	18.78	-3.70×10^{3}
Fog	100	84.06	-3.35	18.78	4.54×10^{-3}

(k) The Specific particle attenuation variation for Average Temperature 2006

Table 4.55: The Specific Particle attenuation variation for Month of January 2006

Size parameter	β	a	b	ρ_i (g/m^3)	α(dB/m)
Air molecules	0.001	314.60	-10.78	15.40	49.59×10^{-12}
	0.01	78.39	-2.18	15.40	202.05×10^{-3}
	0.1	-108.10	4.61	15.40	-32.23×10^{6}
Haze	1	-199.56	7.94	15.40	-535.78×10^{9}
	10	-82.55	3.68	15.40	-1.93×10^{6}
Fog	100	114.37	-3.49	15.40	8.20×10^{-3}

Table 4.56: The Specific particle attenuation variation for Month of February 2006

Size parameter	β	a	b	ρ_i (g/m^3)	α(dB/m)
Air molecules	0.001	314.60	-10.78	30.33	33.35 x 10^{-15}
	0.01	78.39	-2.18	30.33	46.10 x 10^{-3}
	0.1	-108.10	4.61	30.33	-733.25 x 10^{6}
Haze	1	-199.56	7.94	30.33	-116.45 x 10^{12}
	10	-82.55	3.68	30.33	-23.44 x 10^{6}
Fog	100	114.37	-3.49	30.33	770.15 x 10^{-6}

Table 4.57: The Specific Particle attenuation variation for Month of March 2006

Size parameter	β	a	b	ρ_i (g/m^3)	α(dB/m)
Air molecules	0.001	314.60	-10.78	62.77	13.12 x 10^{-18}
	0.01	78.39	-2.18	62.77	9.44 x 10^{-3}
	0.1	-108.10	4.61	62.77	-20.96 x 10^{-9}
Haze	1	-199.56	7.94	62.77	-37.51 x 10^{15}
	10	-82.55	3.68	62.77	-5.18 x 10^{3}
Fog	100	114.37	-3.49	62.77	60.83 x 10^{-6}

Table 4.58: The Specific Particle attenuation variation for Month of October 2006

Size parameter	β	a	b	ρ_i (g/m^3)	α(dB/m)
Air molecules	0.001	314.60	-10.78	14.28	112.14 x 10^{-12}
	0.01	78.39	-2.18	14.28	238.20 x 10^{-3}
	0.1	-108.10	4.61	14.28	-22.75 x 10^{6}
Haze	1	-199.56	7.94	14.28	-294.18 x 10^{9}
	10	-82.55	3.68	14.28	-1.46 x 10^{6}
Fog	100	114.37	-3.49	14.28	10.67 x 10^{-3}

Table 4.59: The Specific Particle attenuation variation for Month of November 2006

Size parameter	β	a	b	ρ_i (g/m^3)	α(dB/m)
Air molecules	0.001	314.60	-10.78	1.43	6.65
	0.01	78.39	-2.18	1.43	35.94
	0.1	-108.10	4.61	1.43	-562.24
Haze	1	-199.56	7.94	1.43	-3.41 x 10^{3}
	10	-82.55	3.68	1.43	-307.86
Fog	100	114.37	-3.49	1.43	32.82

Table 4.60: The Specific Particle attenuation variation for Month of December 2006

Size parameter	β	a	b	ρ_i (g/m^3)	α(dB/m)
Air molecules	0.001	314.60	-10.78	19.94	3.06×10^{-12}
	0.01	78.39	-2.18	19.94	115.04×10^{-3}
	0.1	-108.10	4.61	19.94	-106.06×10^{6}
Haze	1	-199.56	7.94	19.94	-4.16×10^{12}
	10	-82.55	3.68	19.94	-5.00×10^{6}
Fog	100	114.37	-3.49	19.94	3.32×10^{-3}

(L) The Specific Particle attenuation variation for Maximum Temperature 2006

Table 4.61: The Specific Particle attenuation variation for Month of January 2006

Size parameter	β	a	b	ρ_i (g/m^3)	α(dB/m)
Air molecules	0.001	471.15	-12.25	29.43	479.15×10^{-18}
	0.01	130.84	-3.04	29.43	4.48×10^{-3}
	0.1	-67.57	2.33	29.43	-178.66×10^{3}
Haze	1	-309.22	8.87	29.43	-3.29×10^{15}
	10	-202.44	5.98	29.43	-122.93×10^{9}
Fog	100	87.98	-1.88	29.43	152.42×10^{-3}

Table 4.62: The Specific Particle attenuation variation for Month of February 2006

Size parameter	β	a	b	ρ_i (g/m^3)	α(dB/m)
Air molecules	0.001	471.15	-12.25	29.25	516.55×10^{-18}
	0.01	130.84	-3.04	29.25	4.56×10^{-3}
	0.1	-67.57	2.33	29.25	-176.12×10^{3}
Haze	1	-309.22	8.87	29.25	-3.12×10^{15}
	10	-202.44	5.98	29.25	-118.50×10^{9}
Fog	100	87.98	-1.88	29.25	154.19×10^{-3}

Table 4.63: The Specific Particle attenuation variation for Month of March 2006

Size parameter	β	a	b	ρ_i (g/m^3)	α(dB/m)
Air molecules	0.001	471.15	-12.25	70.67	10.47×10^{-21}
	0.01	130.84	-3.04	70.67	312.65×10^{-6}
	0.1	-67.57	2.33	70.67	-1.37×10^{6}
Haze	1	-309.22	8.87	70.67	-7.81×10^{18}
	10	-202.44	5.98	70.67	-23.15×10^{12}

Table4. 64: Month of October 2006 Specific particle attenuation variation

Size parameter	β	a	b	ρ_i (g/m^3)	α(dB/m)
Air molecules	0.001	471.15	-12.25	14.37	2.76 x 10^{-12}
	0.01	130.84	-3.04	14.37	39.63 x 10^{-3}
	0.1	-67.57	2.33	14.37	-33.62 x 10^{3}
Haze	1	-309.22	8.87	14.37	-5.71 x 10^{12}
	10	-202.44	5.98	14.37	-1.69 x 10^{9}
Fog	100	87.98	-1.88	14.37	586.63 x 10^{-3}

Table4. 65: Month of November 2006 Specific particle attenuation variation

Size parameter	β	a	b	ρ_i (g/m^3)	α(dB/m)
Air molecules	0.001	471.15	-12.25	1.59	1.6
	0.01	130.84	-3.04	1.59	31.95
	0.1	-67.57	2.33	1.59	-199.07
Haze	1	-309.22	8.87	1.59	-18.90 x 10^{3}
	10	-202.44	5.98	1.59	-3.24 x 10^{3}
Fog	100	87.98	-1.88	1.59	36.79

Table4. 66: Month of December 2006 Specific particle attenuation variation

Size parameter	β	a	b	ρ_i (g/m^3)	α(dB/m)
Air molecules	0.001	471.15	-12.25	21.89	17.99 x 10^{-15}
	0.01	130.84	-3.04	21.89	11.02 x 10^{-3}
	0.1	-67.57	2.33	21.89	-89.64 x 10^{3}
Haze	1	-309.22	8.87	21.89	-238.91 x 10^{12}
	10	-202.44	5.98	21.89	-20.93 x 10^{9}
Fog	100	87.98	-1.88	21.89	265.90 x 10^{-3}

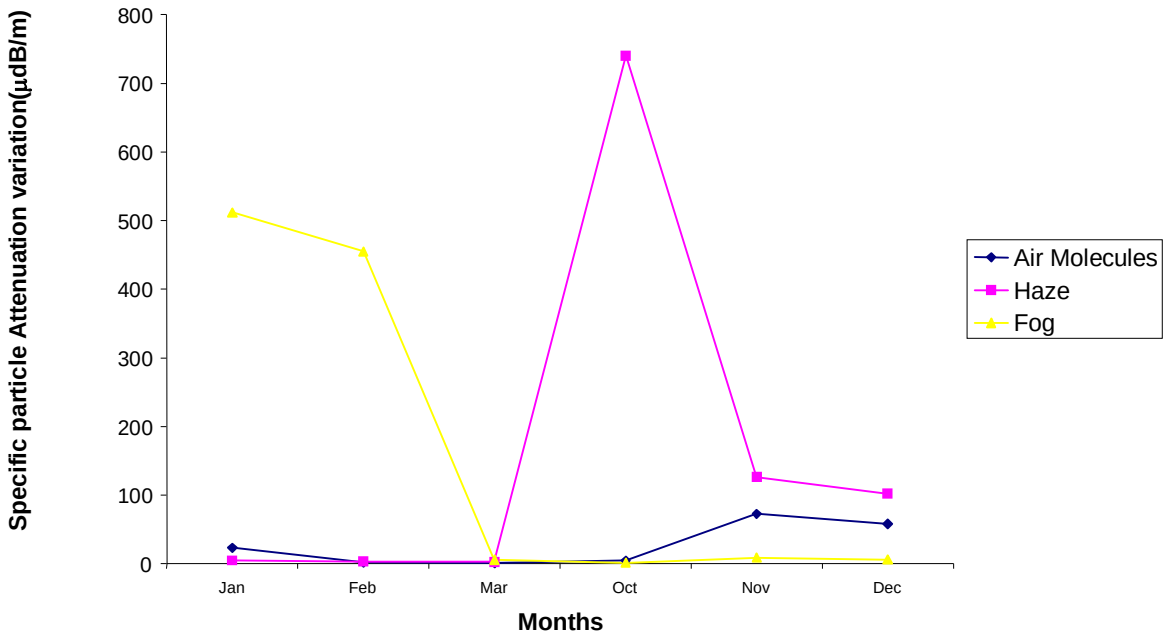

Fig. 4.1: Specific Particle Attenuation variation For 2004: Minimum Temperature

Fig 4.1. Shows that during the months of harmattan, the attenuation is much higher due to haze compared to both fog and air molecules. The maximum specific particle attenuation is 740 µdB and the minimum is approximately 0µdB between February and March. The attenuation due to fog displays a maximum between 510 to 454 µdB between January and March.

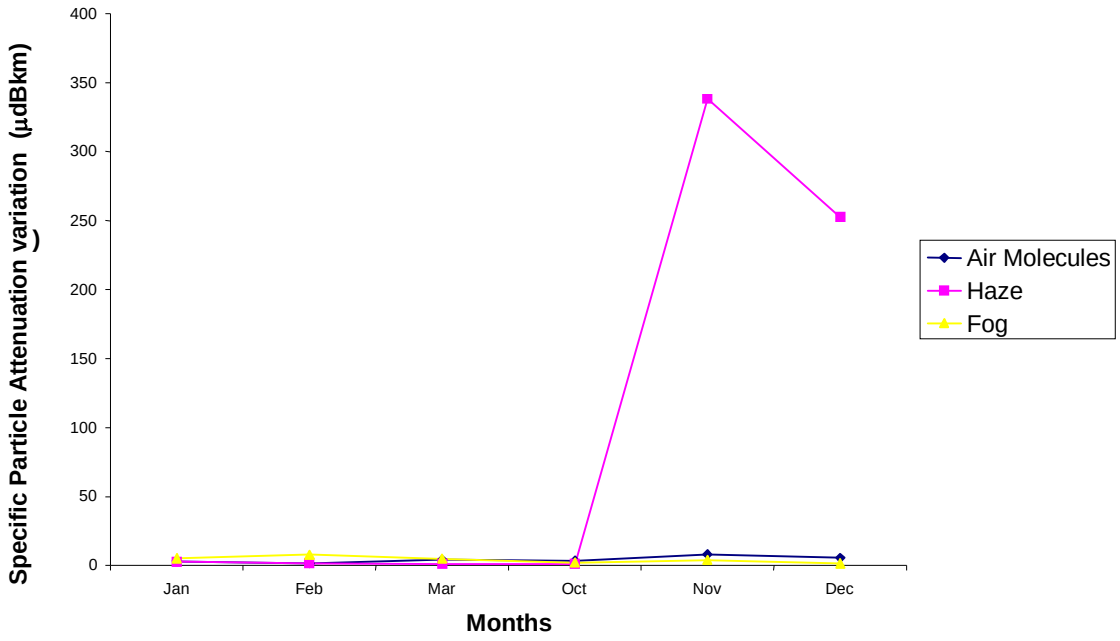

Fig. 4..2: Specific Partilce Attenaution Variation For 2004: Average Temperature

Fig 4. 2. Shows that during the months of harmattan, the attenuation due to haze is much higher compared to both air molecules and fog. The attenuation is 338µdB to 253µdB between November and December. The attenuation due to air molecules display fluctuations between 8µdB and 6µdB respectively between November and December.

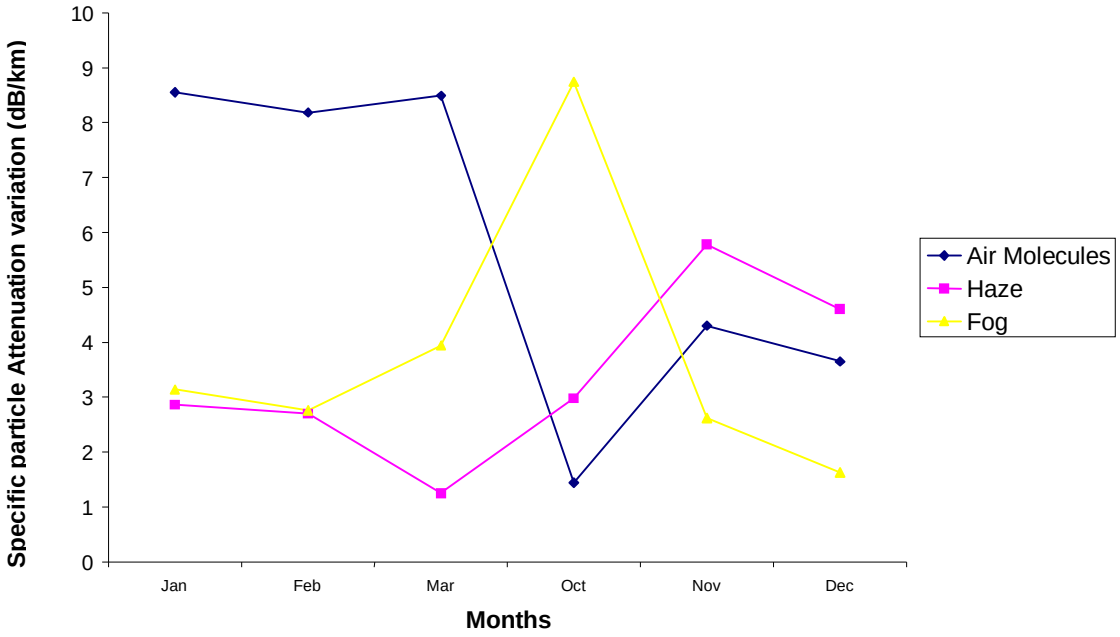

Fig4..3: Specific Particle Attenaution variation For 2004: Maximum Temperature

Fig4.3. Shows that during the months of harmattan, the attenuation is higher due to fog compared to both air molecules and haze. The maximum average values are 9 and 4 dB between October and March; the maximum is 9dB and average is 4dB between October and March; the minimum is 1.8dB in December.

The attenuation due to air molecules displays 2 maxima. Between January and March, the maximum the value is 8.5 dB. While it 4.3 dB in November. The minimum is 1.5 dB in October.

The attenuation due to haze displays a maximum of 5.8dB, which is the maximum, and the average is 3dB between November and October. The minimum is 1.25 dB correspond into the month of March.

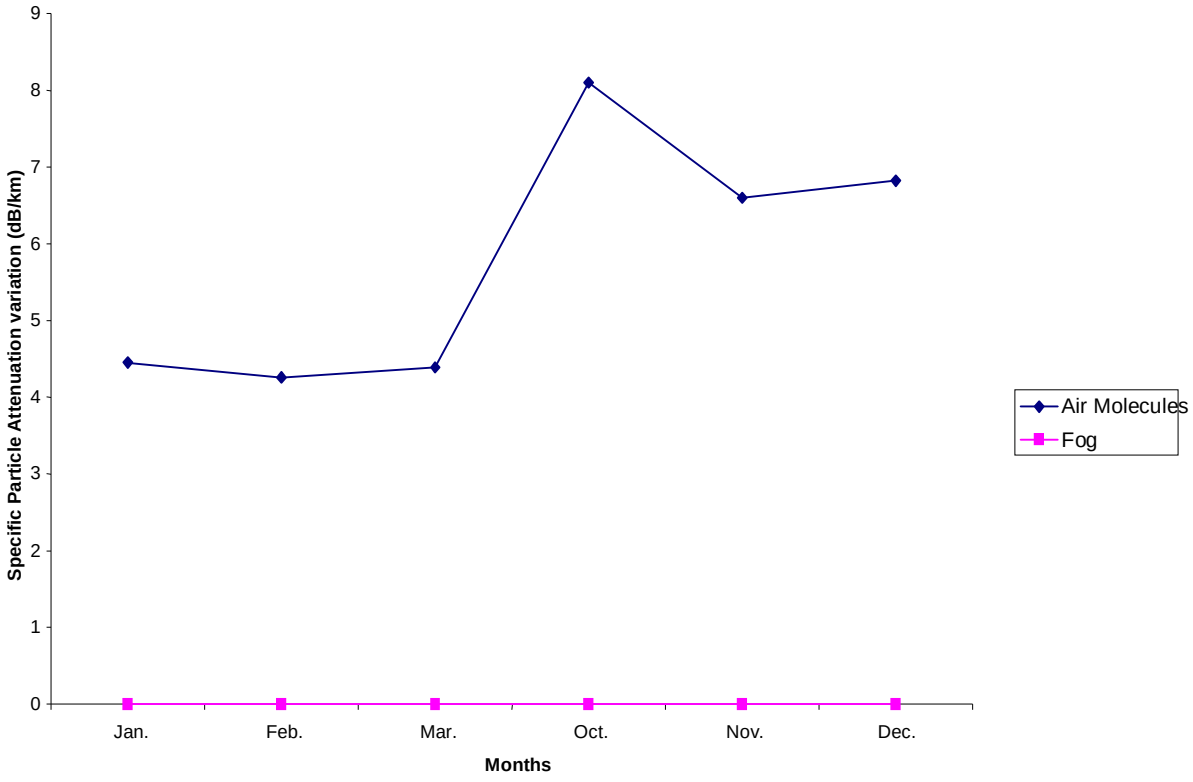

Fig: 4.4 Specific Particle Attenuation variation for 2005 Minimum Temperature

Fig 4.4. Shows that during the months of harmattan, the attenuation due to air molecules is higher compared to fog. The maximum value of attenuation due to air molecules is 8.5dB corresponding to the month of October. While the attenuation due to fog is approximately 0μdB.

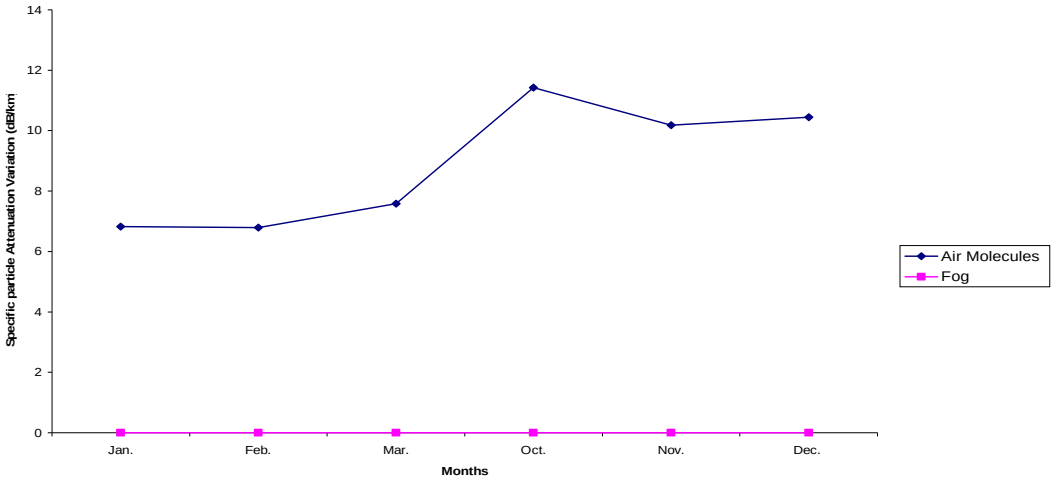

Fig5 : Specific Particle Attenuation variation for 2005 Average Temperature

Fig.4..5: Specific particle Attenuation Variation For 2005: Average Temperature

Fig5.5. Shows that during the months of harmattan, the attenuation due to air molecules is higher than that due to fog. The maximum attenuation due to air molecules is 11.5dB corresponding to the month of October.

While the attenuation due to Fog is approximately 0dB in October.

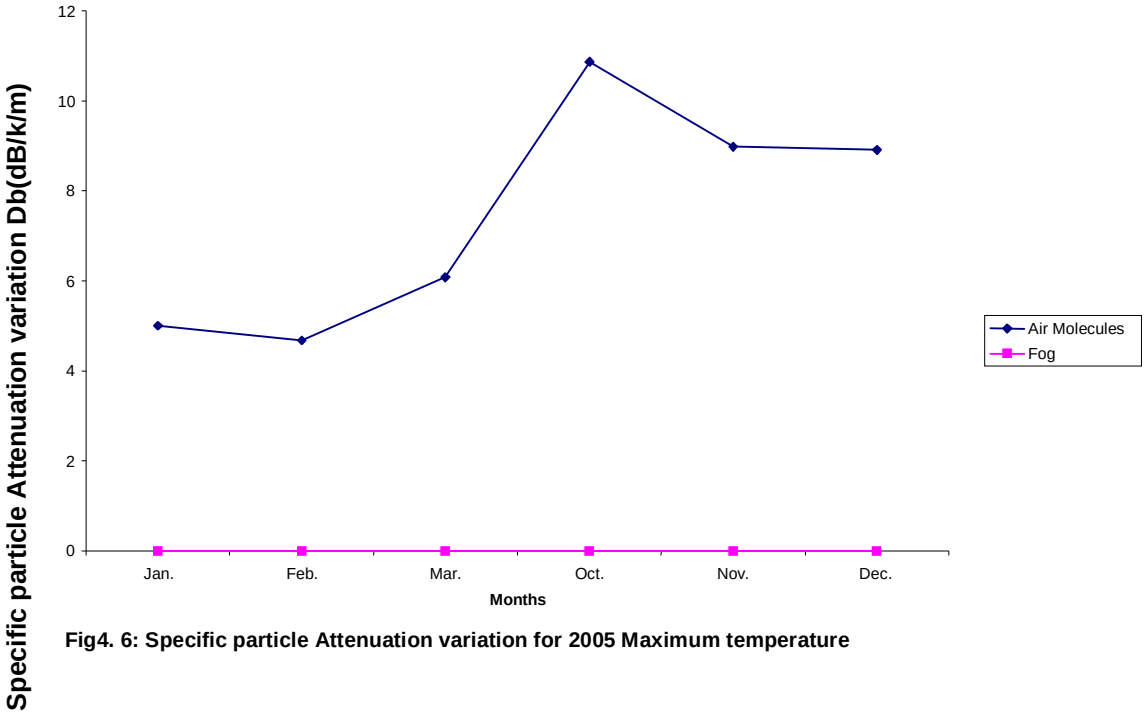

Fig4. 6: Specific particle Attenuation variation for 2005 Maximum temperature

Figure 4.6: Shows that during the months of harmattan, the attenuation air molecules is higher compared to fog. The maximum attenuation is 11.8dB corresponding to the month of October .

The attenuation to fog is approximately 0.dB .

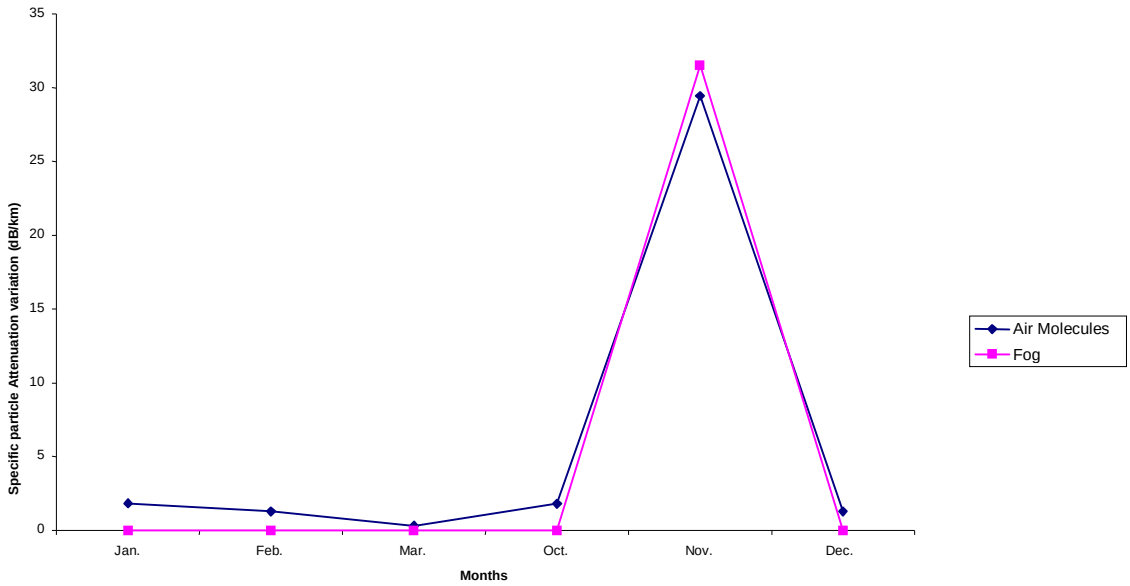

Fig4. 7: Specific particle Attenuation variation for 2006 Minimum Temperature

Fig 4.7. Shows that during the months of harmattan, the attenuation due to fog is higher compared to air molecules . The maximum attenuation is 33dB corresponding to the month of November. While the attenuation due to air molecules displays a maximum of 30dB in November .

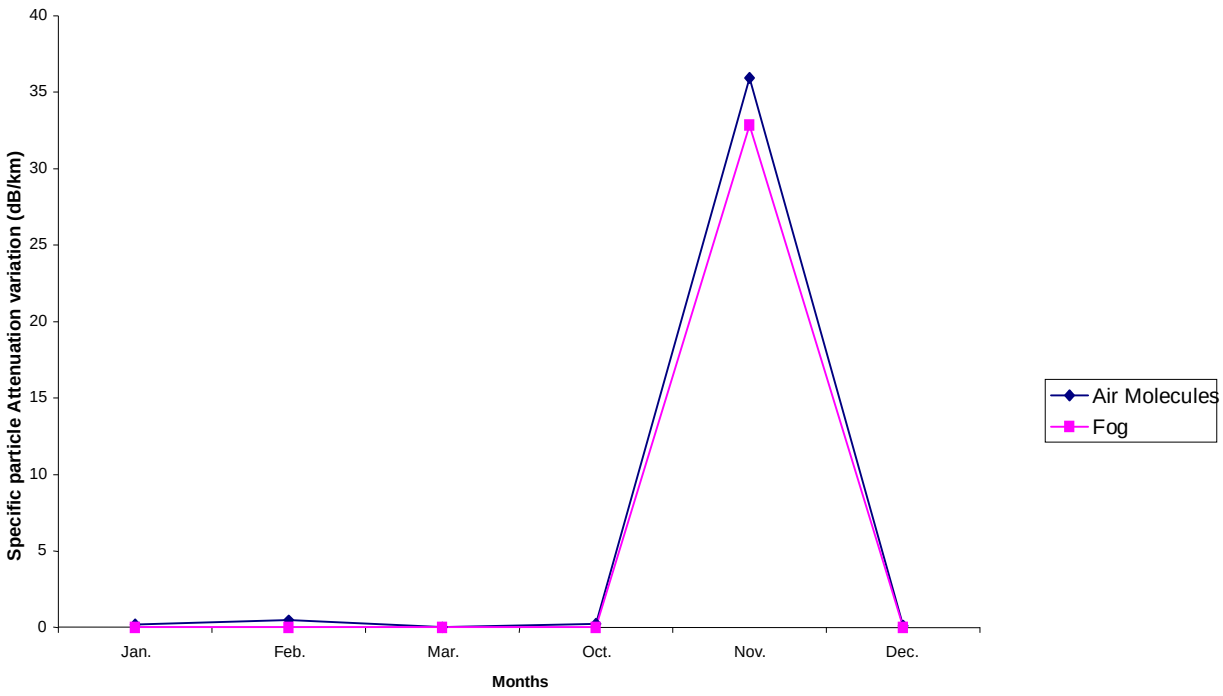

Fig4. 8: Specific particle Attenuation variation for 2006 Average Temperature

Fig 4.8. Shows that during the months of harmattan, the attenuation due to air molecules is higher compared to fog. The maximum attenuation is 37dB corresponding to the month of November. While the attenuation due to fog displays a maximum of 35dB in November.

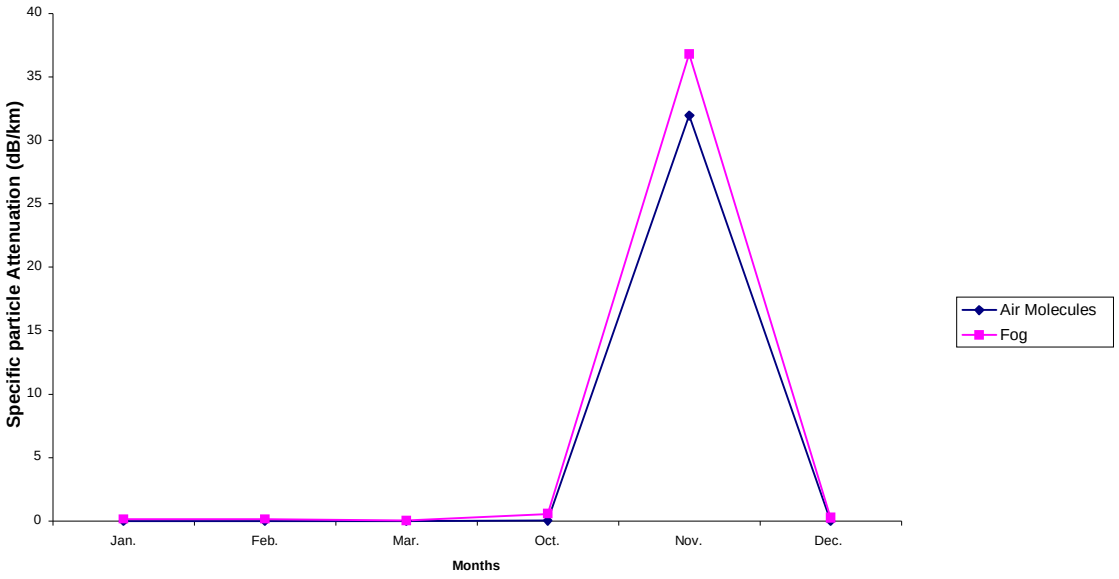

Fig 4.9: Specific particle Attenuation variation for 2006 Maximum Temperature

Fig4.9. Shows that during the months of harmattan, the attenuation due to fog is higher compared to air molecules . The maximum attenuation is 38dB corresponding to the month of November. While attenuation due to air molecules displays a maximum of in November. These results show that the lower values of attenuation represent higher visibility values of 1000m or 15000m, while the upper values representing the lower visibility value of 200m or 300m. The calculated specific particle attenuation variation has been found to give fairly good agreement with the following results.

4.3 PATHLOSS ANALYSIS FROM FIELD DATA

The losses in signal strength that occur during transmission from the T_X antenna to the R_X antenna are given by the path loss, while the receive power is the result of the path loss phenomenon. The path loss was obtained from the effective isotropic radiated power (EIRP) using the expression:

$$Lp = EIRP - S_R \text{ ---------- (4.3)}$$

Where,

S_R is the measured received signal strength.

4.3.1 Free-space Path loss Model (Analytical)

The received power level, P_R at the receiving antenna, MS can be calculated analytically as follows:

For an isotropic antenna in free space:

$$P_R = \frac{P_T}{4\pi d^2} \quad (4.4)$$

For an isotropic antenna radiating uniformly in all directions (spherical pattern), the power density, P_R is given by the equation (4.4)

When a directional transmitting antenna with a power gain factor G_T is used, the power density at the receiver site is G_T times equation (4.4), i.e.

$$P_{R,(direc)} = P_R G_T = \frac{P_T G_T}{4\pi d^2} \quad (4.5)$$

If the receiving antenna has an aperture area A_R then the power captured by the receiver is $\overline{P}_{R,(direc)}$ times A_R

i.e.

$$\overline{P}_{R,(direc)} = \frac{P_T G_T A_R}{4\pi d^2} \quad \text{----------(4.6)}$$

The aperture area is related to the gain of the receiving antenna and the wavelength by (20):

$$G_{R,} = \frac{4\pi A_R}{\lambda^2} \quad \text{----------(4.7)}$$

Where

$\lambda = \frac{C}{f}$, and f = the transmission frequency in Hz

$C = 3X10^8 m/s$ is the free-space speed of propagation for electromagnetic waves, and is the wavelength in m.

Now the total received power P_R is:

$$P_R = A_R P_R \quad \text{----------(4.8)}$$

Substituting for A_R and P_R from the above, we have:

$$P_R = \left[\frac{\lambda}{4\pi d}\right]^2 P_T G_T G_R \quad \text{----------(4.9)}$$

The path propagation loss, L_P which denote the loss associated with propagation of e.m. waves from the transmitter to the receiver, is given by:

$$L_P = \left[\frac{\lambda}{4\pi d}\right]^2 \quad \text{----------(4.10)}$$

It can be seen that this loss depends on the carrier frequency and the T-R separation distance. The product $P_T G_T$ is called the Equivalent Isotopic Radiated Power (EIRP). If

P_T and P_R are expressed in same unit of dBm in equation (4.9), then P_R and L_P can be expressed in dBm and dB (20) as follows:

$$P_P = 20log\left[\frac{\lambda}{4\pi d}\right] + P_T + G_T + G_R(dBm) \text{ ----------} \quad (4.11)$$

$$L_P = 20log\left[\frac{4\pi d}{\lambda}\right](dB) \text{ ----------} \quad (4.12)$$

4.3.2 ANALYSIS OF THE COST- 231 HATA MODEL

The COST- 231 Hata path loss model for urban areas is:

$$L_P = A + B\log(d) + C \text{ ……..……} \quad (4.12)$$

$$A = 46.3 + 33.9\log(f_c) - 13.82\log(h_b) - a(h_m) \text{ ……..…..} \quad (4.13)$$

$$B = 44.9 - 6.55\log(h_b) \text{ ……...} \quad (4.14)$$

$$a(h_m) = 3.2[\log(11.75h_m)]^2 - 4.97 \text{ ……..} \quad (4.15)$$

$C = 3dB$, $f_c = 900MHz$, $h_m = 1.5m$

Substituting the above parameters into equation (4.12) to have:

$$L_P = 46.3 + 33.9\log(900) - 13.82\log(h_b) - \left[3.2(\log 17.63)^2 - 4.97\right] + \left[44.9 - 6.55\log(h_b)\right]\log d + 3$$

$$L_P = 149.45 - 13.82\log(h_b) + \left[44.9 - 6.55\log(h_b)\right]\log d \text{ ……} \quad (4.16)$$

For base stations of height 32m, substituting $h_b = 32m$ into equations (4.16):

$$L_P = 149.45 - 13.82\log(32) + \left[44.9 - 6.55\log(32)\right]\log d \text{ ……..……...} \quad (4.17)$$

$$L_P = 128.65 + 35.05\log d \text{ …… .. … … ..… ……..…} \quad (4.18)$$

For base stations of height 34m, substituting the value of $h_b = 34m$ into equation (4.16):

$$L_P = 149.45 - 13.82\log(34) + [44.9 - 6.55\log(34)]\log d \quad \text{.............................} (4.19)$$

$$= 128.28 + 34.87\log d \quad \text{...} (4.20)$$

The average of equations (4.18) and (4.20) is:

$$= 128.5 + 35\log d \quad \text{..} (4.21)$$

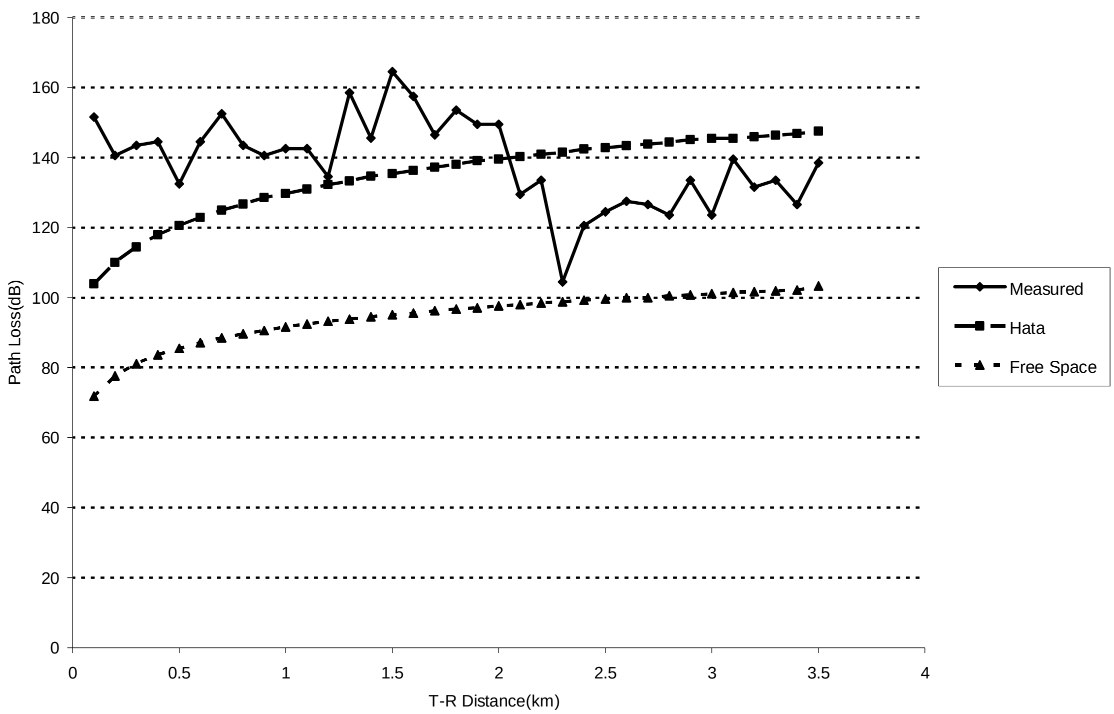

Figure 4.10: PATH LOSS VARIATION ON DIGUEL ROAD FOR MARCH,2006

.

.

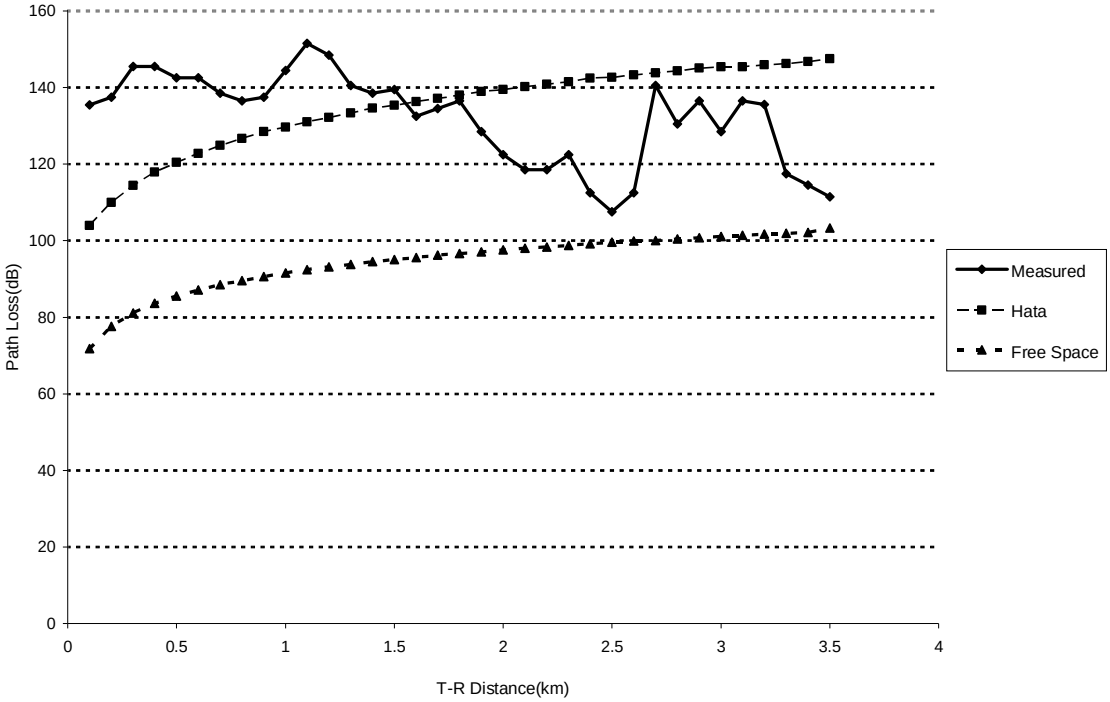

Figure 4.11: PATH LOSS VARIATION ON MOURSAL ROAD FOR MARCH, 2006

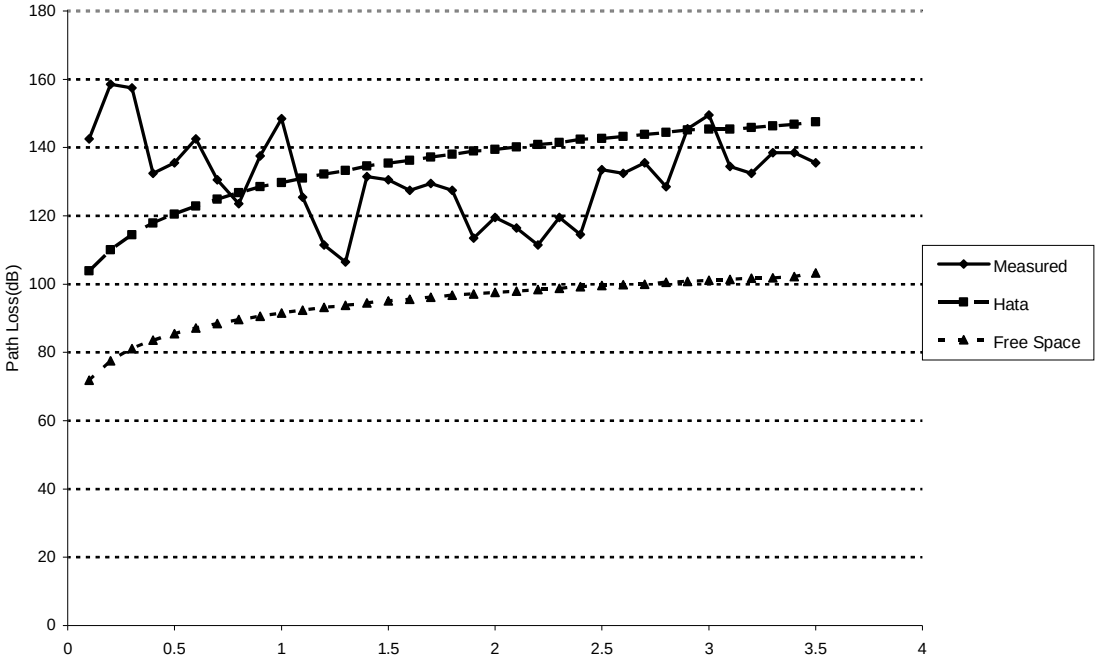

Figure 4.12: PATH LOSS VARIATION ON DIGUEL ROAD FOR FEBRUARY,2006

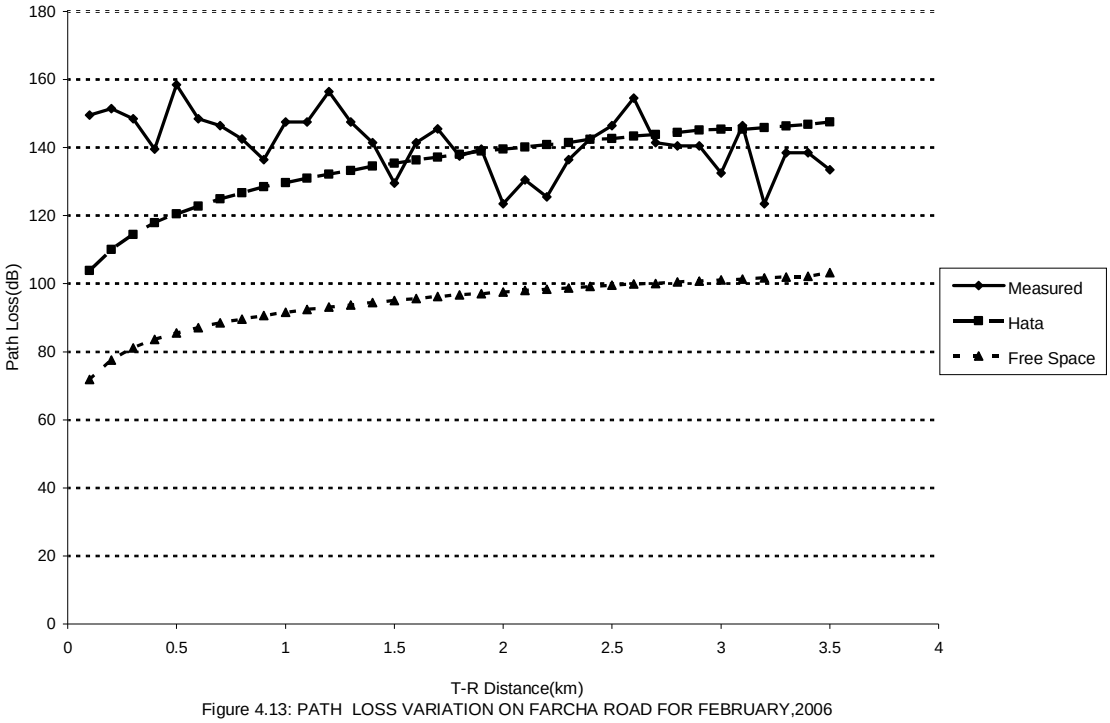

Figure 4.13: PATH LOSS VARIATION ON FARCHA ROAD FOR FEBRUARY,2006

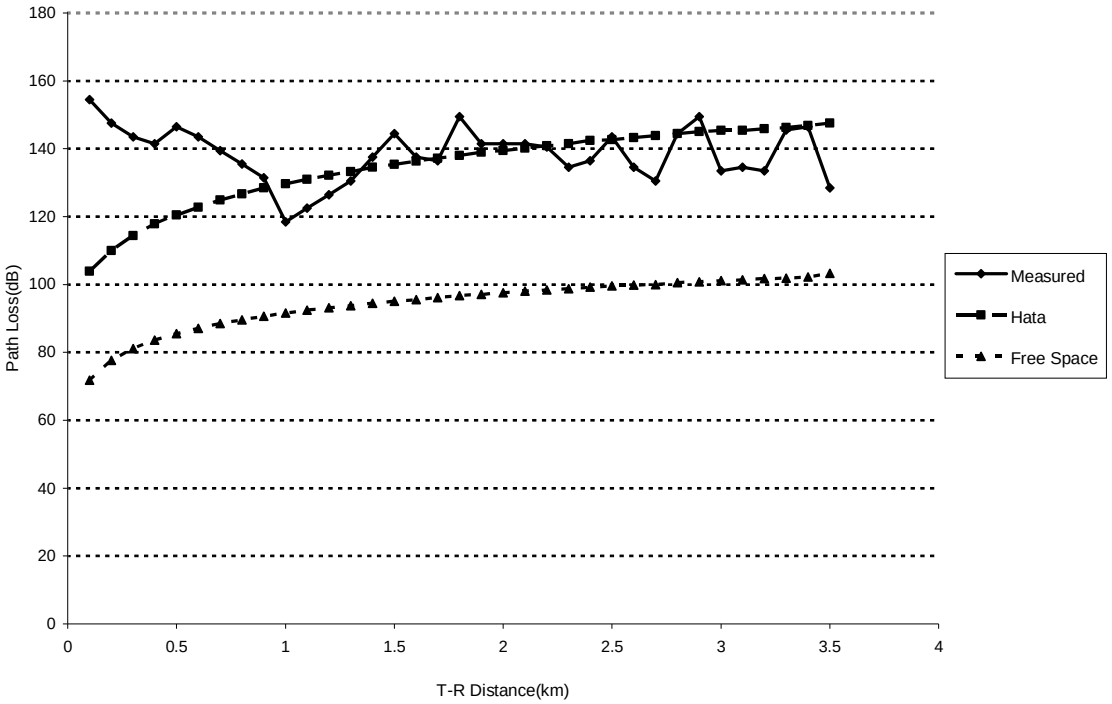

Figure 4.14: PATH LOSS VARIATION ON MOURSAL ROAD FOR JANUARY,2006

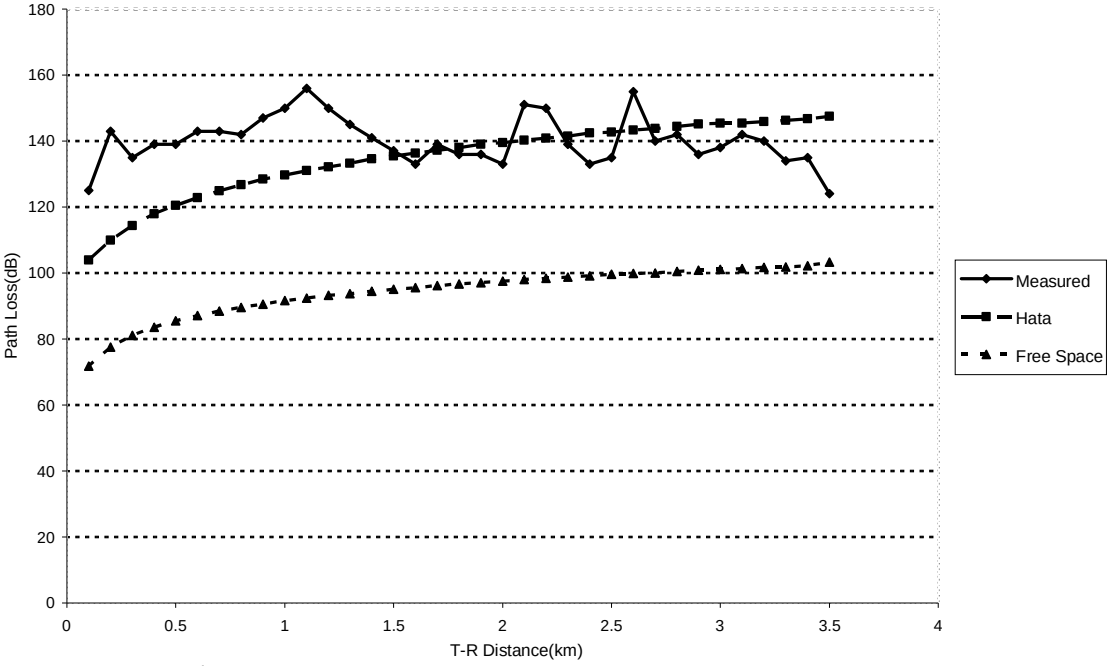

Figure 4.15: PATH LOSS VARIATION ON CHAGOUA ROAD FOR NOVEMBER,2005

The graphs in Figures (4.10) to (4.12) show that below 1.5km Hata model under predicts the path loss from measurement results while from 2km and above it overestimates the

path loss. Thus, these variations may be due to interference from nearby base stations, which are not considered in the measurement, and also the improper use of equipments. It can also be due to varying and environmental factors at the various base stations. The graphs in Figures (4.13) to (4.15) show that from 2km and above, the Hata model provides a closer prediction of the path loss to that obtained from the measurement. It should be noted that in 2006, on all the sample of roads under investigations, the path loss variation falls in the range between 71.8dB and 158.9dB. These variations of path loss and consequently received power can be explained by the increase of dust particles in the air. A closer look at Table 4.3 shows that harmattan dust density in air displays fluctuation in the range 14.08 g/m^3 to 70.67g/m^3 between January and March 2006. A closer look at Table 4.2 shows that harmattan dust density in air increases from 16.53g/m^3 to 66.88g/m^3 between November and February 2005.The slightly lower precipitation rate difference between 2005 and 2006 is responsible for the differences in the path losses by a magnitude of about 2 dB.

4.4 ANALYSIS OF VISIBILITY EFFECTS ON SIGNAL WAVELENGTH

To calculate atmospheric losses (in dB/km), equation 4.22 and 4.23 are used and the results displayed in the Tables that follows.

$q = 0.585V^{1/3}$ ----------(4.22)

$$\sigma = \frac{3.91}{v}\left(\frac{\lambda}{\lambda_{GSM\,900\,MHZ}}\right)^{-q}$$ ----------(4.23)

which λ_{900MHZ}…….. $\lambda_{1800MHZ}$.

Table4. 67: range of wavelengths in the GSM frequency band.

Frequency (MHZ)	Wave length (cm)
900	33
1000	30
1100	27
1200	25
1300	23
1400	21
1500	20
1600	18
1700	17
1800	16

Table4. 68: Atmospheric losses (2004)

Visibility(km)	**dB/km 30cm**	**dB/km 27cm**	**dB/km 25cm**	**dB/km 23cm**	**dB/km 21cm**	**dB/km 20cm**	**dB/km 18cm**	**dB/km 17cm**	**dB/km 16cm**	**Weather**
0.3	12.55	12.05	11.69	11.32	10.92	10.72	10.28	10.06	9.82	Fog
0.6	6.21	5.90	5.68	5.46	5.22	5.09	4.84	4.70	4.57	
0.8	4.64	4.38	4.20	4.02	3.82	3.72	3.52	3.41	3.30	Mist
1	4.13	4.39	4.59	4.82	5.08	5.22	5.55	5.74	5.95	Haze

Table 4 69 the size distribution of the scattering particles

Visibility(Km)	q
0.2	0.34
0.3	0.39
0.6	0.49
0.8	0.54
1	0.58
1.5	0.66

Table 4.70: Atmospheric losses (2005)

Visibility(km)	dB/km 30cm	dB/km 27cm	dB/km 25cm	dB/km 23cm	dB/km 21cm	dB/km 20cm	dB/km 18cm	dB/km 17cm	dB/km 16cm	Weather
0.2	18.94	18.29	17.83	17.35	16.84	16.57	16.00	15.70	15.39	Fog
0.3	12.55	12.05	11.69	11.32	10.92	10.72	10.28	10.06	9.82	
0.8	4.64	4.38	4.20	4.02	3.82	3.72	3.52	3.41	3.30	Mist
1	4.13	4.39	4.59	4.82	5.08	5.22	5.55	5.74	5.95	Haze

Table 4.71: Atmospheric losses (2006)

Visibility(km)	dB/km 30cm	dB/km 27cm	dB/km 25cm	dB/km 23cm	dB/km 21cm	dB/km 20cm	dB/km 18cm	dB/km 17cm	dB/km 16cm	Weather
0.3	12.55	12.05	11.69	11.32	10.92	10.72	10.28	10.06	9.82	Fog
0.6	6.21	5.90	5.68	5.46	5.22	5.09	4.84	4.70	4.57	
0.8	4.64	4.38	4.20	4.02	3.82	3.72	3.52	3.41	3.30	Mist
1	4.13	4.39	4.59	4.82	5.08	5.22	5.55	5.74	5.95	Haze
1.5	2.44	2.28	2.17	2.05	1.93	1.87	1.74	1.68	1.61	

Table4. 72: Atmospheric losses (2004)

Visibility(km)	**dB/km 30cm**	**dB/km 27cm**	**dB/km 25cm**	**dB/km 23cm**	**dB/km 21cm**	**dB/km 20cm**	**dB/km 18cm**	**dB/km 17cm**	**dB/km 16cm**	**Weather**
0.3	13.03	13.03	13.03	13.03	13.03	13.03	13.03	13.03	13.03	Fog
0.6	6.45	6.38	6.33	6.28	6.22	6.19	6.13	6.09	6.06	Mist
0.8	4.74	4.60	4.49	4.38	4.26	4.20	4.07	4.00	3.93	
1	4.10	4.32	4.49	4.68	4.90	5.02	5.29	5.44	5.61	Haze

Table 4.73: the size distribution of the scattering particles

Visibility(Km)	q
0.2	0
0.3	0
0.6	0.1
0.8	0.3
1	0.5
1.5	0.58

$$\sigma = \frac{3.91}{v}\left(\frac{\lambda}{\lambda_{GSM\,900\,MHZ}}\right)^{-q}$$

Table4. 74: Atmospheric losses (2005)

Visibility(km)	dB/km 30cm	dB/km 27cm	dB/km 25cm	dB/km 23cm	dB/km 21cm	dB/km 20cm	dB/km 18cm	dB/km 17cm	dB/km 16cm	Weather
0.2	19.55	19.55	19.55	19.55	19.55	19.55	19.55	19.55	19.55	Fog
0.3	13.03	13.03	13.03	13.03	13.03	13.03	13.03	13.03	13.03	Mist
0.8	4.74	4.60	4.49	4.38	4.26	4.20	4.07	4.00	3.93	
1	4.10	4.32	4.49	4.68	4.90	5.02	5.29	5.44	5.61	Haze

Table4. 75: Atmospheric losses (2006)

Visibility(km)	dB/km 30cm	dB/km 27cm	dB/km 25cm	dB/km 23cm	dB/km 21cm	dB/km 20cm	dB/km 18cm	dB/km 17cm	dB/km 16cm	Weather
0.3	13.03	13.03	13.03	13.03	13.03	13.03	13.03	13.03	13.03	Fog
0.6	6.45	6.38	6.33	6.28	6.22	6.19	6.13	6.09	6.06	Mist
0.8	4.74	4.60	4.49	4.38	4.26	4.20	4.07	4.00	3.93	
1	4.10	4.32	4.49	4.68	4.90	5.02	5.29	5.44	5.61	Haze
1.5	2.46	2.32	2.21	2.11	2.00	1.94	1.83	1.77	1.71	

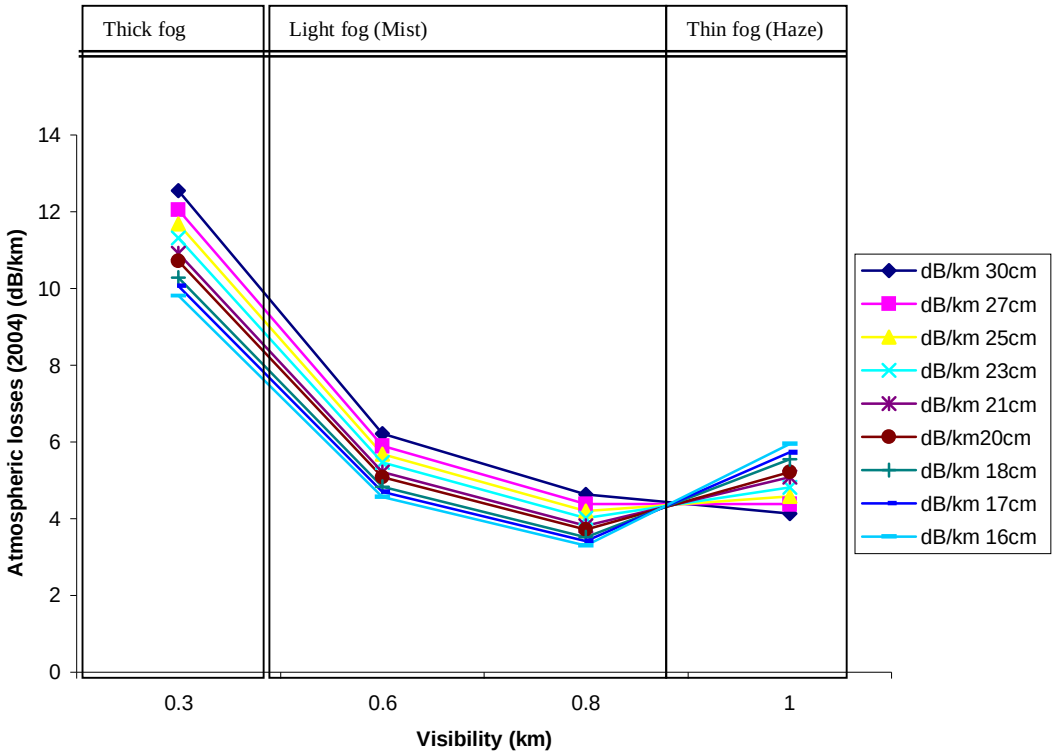

Fig 4.16: Graph of Atmospheric losses for 2004

In Fig4.16. The wavelengths in color show amount of atmospheric losses as functions of visibility. . For visibility (< 800m) GSM wavelengths, thick fog and light fog are the primary weather conditions, which can cause link outages. This is demonstrated in Fig 26.. The Fig. 26 shows a plot of the atmospheric losses. The technical definition of visibility or visual range is the distance that light decreases to 2% of the original power, or qualitatively, visibility is the distance at which it is just possible to distinguish a dark object against the horizon. The atmospheric losses- visibility curve was calculated for 900 MHz – 1800 MHz. In Fig. 26, the atmospheric losses decrease when the visibility

increases. The maximum value of atmospheric losses is 12.5 dB and the minimum 3.7. When look at thin fog the atmospheric losses increase slightly from 4.1 to 6 dB/Km when the visibility increases from 0.8 to 1.

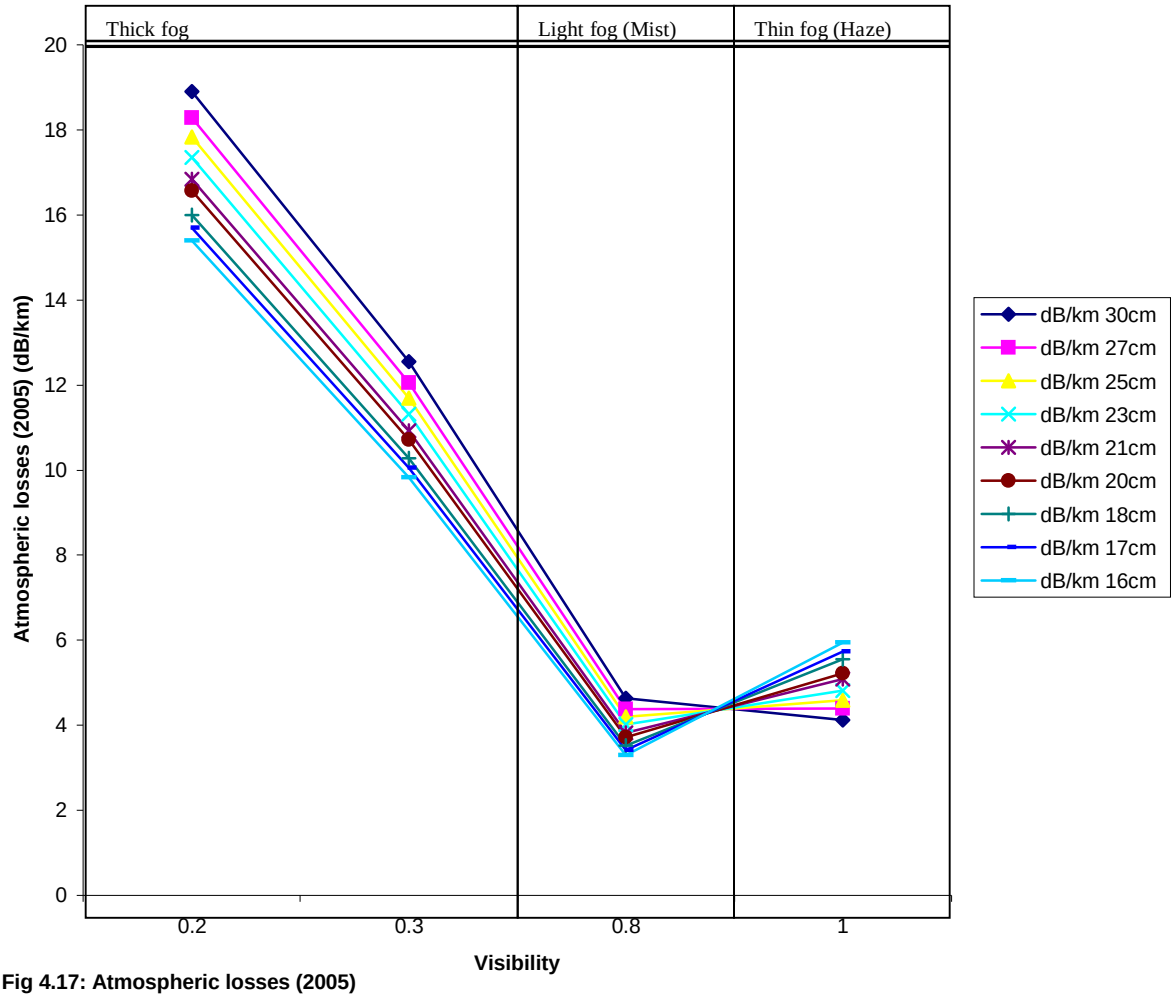

Fig 4.17: Atmospheric losses (2005)

In **Fig 4.17,** the wavelengths in colors show the amount of atmospheric losses as function of visibility.. For visibility (< 300m), thick fog is the primary weather condition that affects the propagation of microwaves. Secondary weather conditions are light fog and thin fog . The atmospheric loses-visibility curve was calculated for 900MHZ-1800MHZ. The atmospheric losses decrease when the visibility increases. The maximum

value of atmospheric losses is 18.9 dB/Km and the minimum is 3.3 dB/Km. The atmospheric losses increase slightly from 4.1to 6. dB/km when the visibility increase for thin fog weather condition.

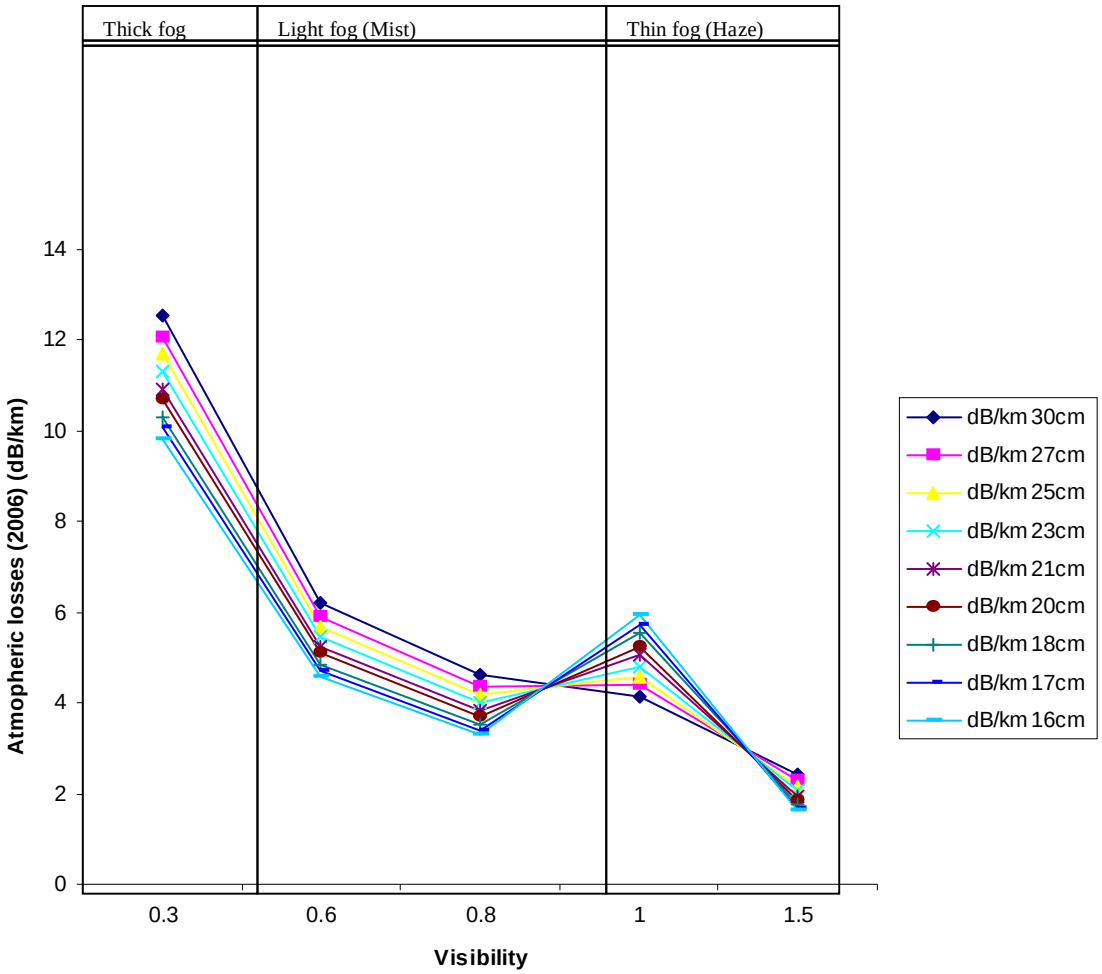

Fig 4.18: atmospheric losses (2006)

In **Fig.4.18,** the wavelengths in colour show amount of atmospheric losses as function of visibility. . For visibility (< 300m), thick fog is the primary weather condition that affects the propagation of microwave signals. Secondary weather conditions are light fog and thin fog . The atmospheric losses-visibility curve was calculated for 900MHz-1800MHz. The atmospheric losses decrease when the visibility increases. The maximum value due to atmospheric losses is 13.03 dB and the minimum is 1.71 dB/km.

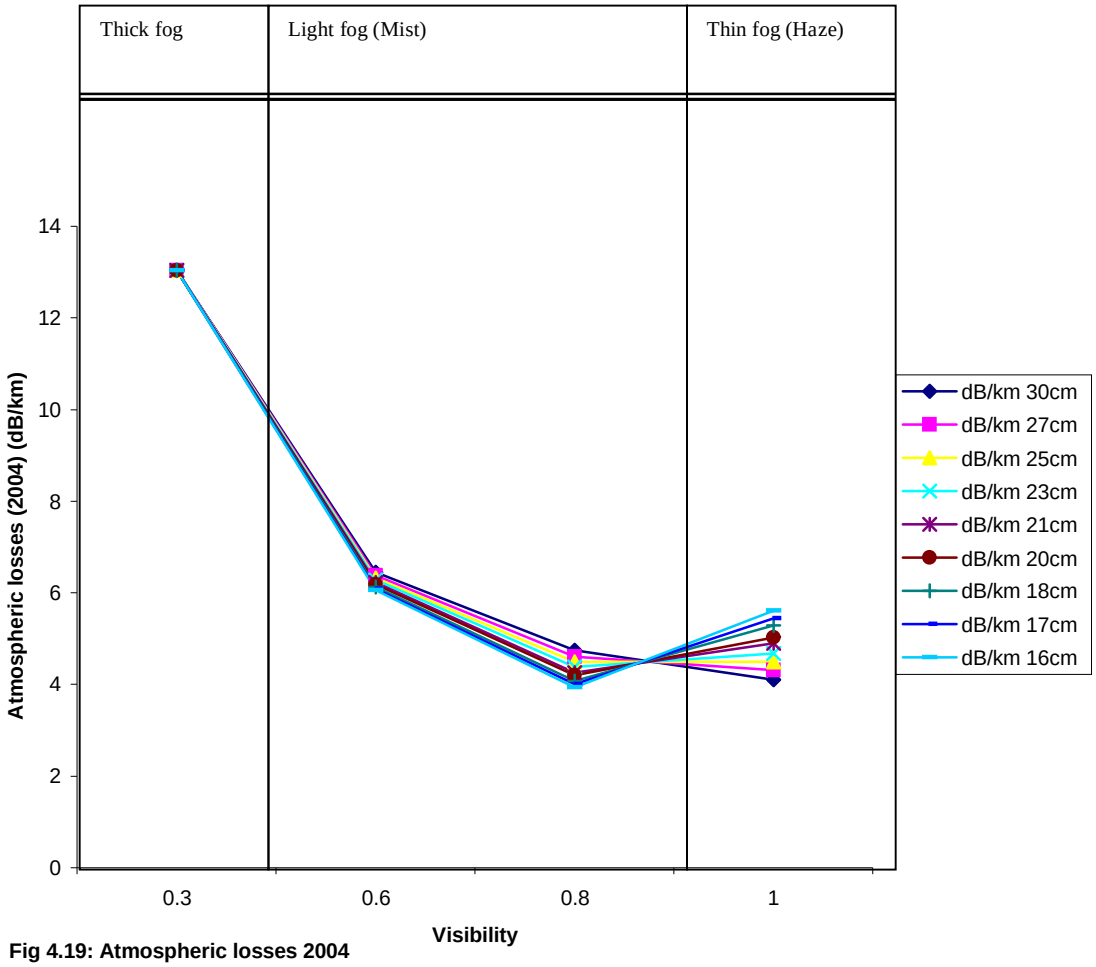

Fig 4.19: Atmospheric losses 2004

In **Fig. 4.19**, the wavelengths in colour show amount of atmospheric losses as function of visibility. . For visibility (< 300m), thick fog is the primary weather condition that affects the propagation of microwaves. Secondary weather conditions are light fog and thin fog . The atmospheric losses-visibility curve was calculated for 900MHz-1800MHz. The atmospheric losses decrease when the visibility increases. The maximum value due to atmospheric losses is 13 dB and the minimum is 3.8 dB/km.

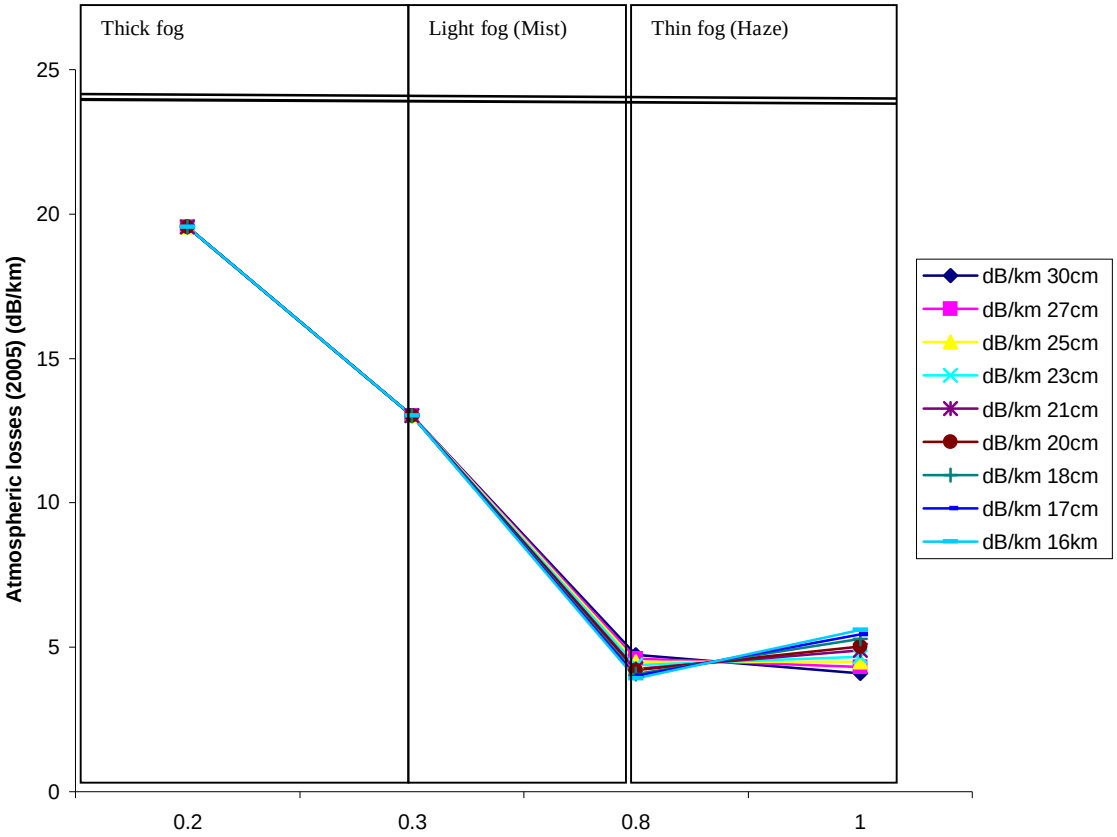

Fig 4.20: Atmospheric losses (2005)

In **Fig4.20**. the wavelengths in colour show amount of atmospheric losses as function of visibility. The atmospheric losses decrease when the visibility increases. The maximum value due to atmospheric losses is 13 dB and the minimum is 3.93 dB/km. While for thin fog the atmospheric losses increases from 4.1 to 5.6dB/km when the visibility increases from 0.8 to 1km.

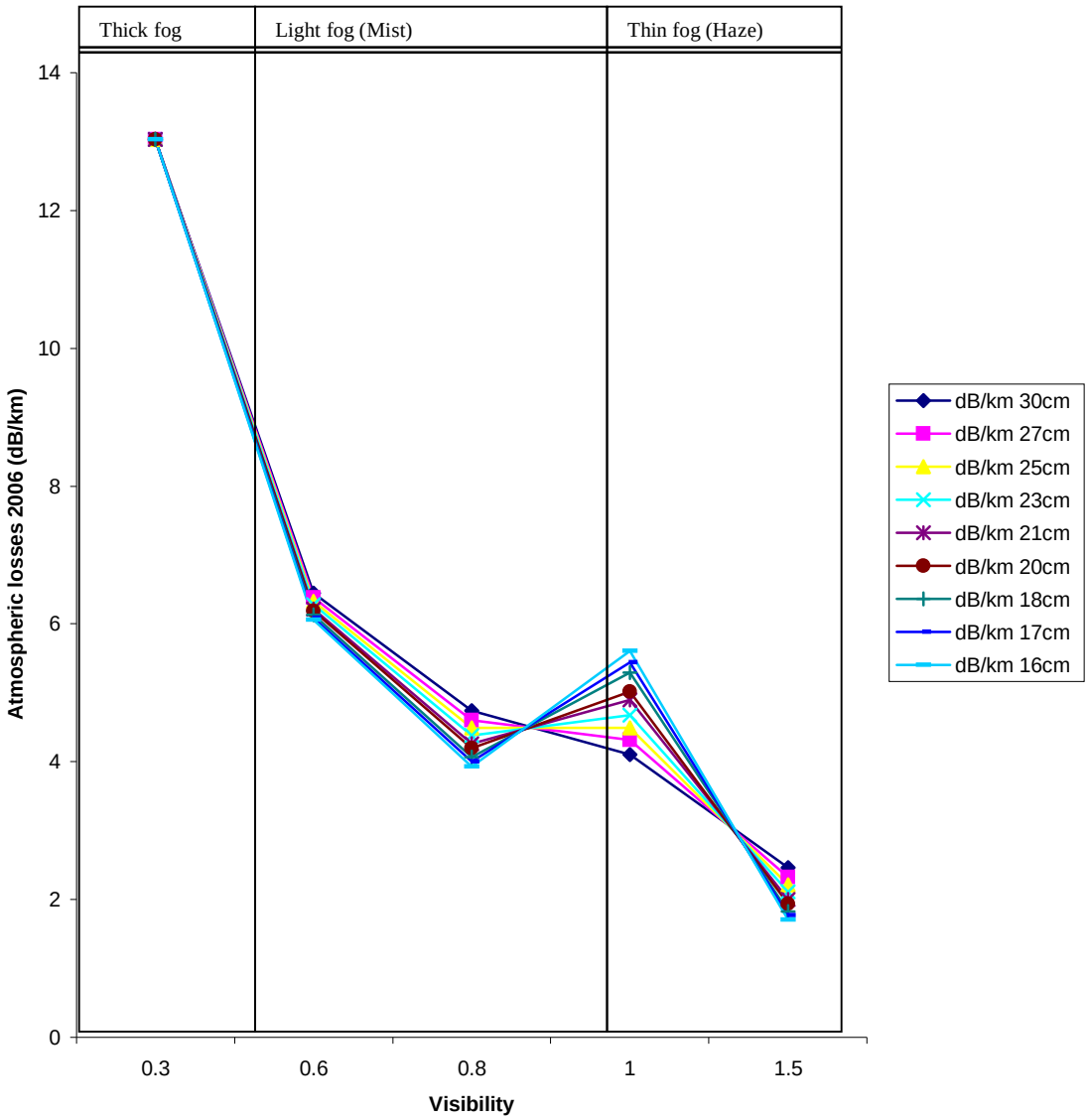

Fig 4.21: Atmospheric losses (2006) (dB/km)

In Fig. 4.21: The wavelengths in colour show amount of atmospheric losses as function of visibility. . For visibility (< 300m), thick fog is the primary weather condition that affects the propagation of microwave signal. Secondary weather conditions are light fog (mist) and thin fog (haze). The atmospheric losses-visibility curve was calculated for 900MHZ-1800MHZ. The atmospheric losses decrease when the visibility increases. The maximum value due to atmospheric losses is 19.5 dB and the minimum is 3.9 dB/km.

The atmospheric losses increase slightly from 4.1dB to 5.6dB when the visibility increases for thin fog (Haze) weather condition.

4.5 DISCUSSION OF RESULTS

In the course of the study, it was identified that precipitates that adversely affects propagation within the period include air molecules, fog and haze.

The values of the specific particle attenuation variation for 2004 indicated that the maximum attenuation occurs at periods corresponding to maximum temperatures with a value of 9 dB as shown in Fig 4.3. .During minimum and average temperatures, the attenuation is in micro decibels as shown in Fig 4.1 - 4.2. In comparison to 2004, the year 2005 displayed the most adverse effect of harmattan as the values of the specific particle attenuations are all in the decibel range at all temperatures (minimum, average and maximum). The values range between 11..8dB at maximum temperature to , 11.5dB at average temperature and 8.5 dB at minimum temperature. (see fig 4.4, 4.5 and 4.6). The trend for 2005 continues in the year 2006, as the values of the specific particle attenuation for all temperatures are in the magnitude between 38dB at maximum temperature, 37dB at average temperature and 33dB at minimum temperatures.

These aggregate specific particles attenuations on radio signals manifest themselves as path loss at the receiver end .From the field data obtained and analysis carried out, for the year 2006 it could be established that the resultant path losses on the transmitter - receiver network of a mobile operator fall in the range between 59.5dB to 167.5dB..This corroborates increases in specific particle attenuation observed for 2005 and 2006 which shows an increasing trend due to precipitate activity.

A closer look at the results obtained from the three different methods indicate that the path losses are higher than both specific particle attenuation and constituent atmospheric losses. The atmospheric losses display a similar pattern in all cases. The difference, however is that there is shift in corresponding values of the loss depending on the visibility and wavelength

4.6 STATIATICAL ANALYSIS OF RESULTS

A statistical analysis was made to determine the variations with road using the following parameter of path losses;

- ✓ Extreme maximum value of path loss.
- ✓ Extreme miniimum value of path loss.

Mean prediction error $\mu_e = \frac{Measuredpathloss - CoompuutedAtmosphericlosses}{n}$ -----(4.6)

Where

n = no of measurements intervals----------(4.7)

Standard Deviation of the men prediction error (σ_e) $\sqrt{\frac{\sum d^2}{n-1}}$ ----------(4.8)

Table 4.76: Path loss prediction statistics for the sample of roads.

Wavelength (cm)	Diguel Road		Moursal Road		Farcha Road		Chagoua Road	
	μ_e	**σ_e**	**μ_e**	**σ_e**	**μ_e**	**σ_e**	**μ_e**	**σ_e**
30	136.6	157.79	130.93	151.46	139.67	161.31	135.24	151.45
27	136.82	158.02	131.22	151.77	139.66	161.31	135.27	151.47
25	136.94	158.18	131.42	151.99	139.66	161.31	137.89	154.49
23	137.09	158.33	131.62	152.20	139.65	161.30	135.30	151.51
21	137.24	158.50	131.83	152.43	139.64	161.28	135.31	151.52
20	137.31	158.58	131.94	152.55	139.64	161.27	135.32	151.52
18	138.95	158.74	132.16	152.79	139.62	161.25	135.33	151.53
17	137.52	158.82	132.27	152.91	139.61	161.24	135.33	151.53
16	137.59	158.90	132.27	153.03	139.59	161.22	135.33	151.52
Ave.	137.34	158.42	131.74	153.12	139.63	161.27	135.59	151.50

Table 4.76 presents the path loss obtained from measurements result compared with atmospheric loss computed. The mean prediction values 139.63 dB,137.34dB, 135.59dB and 131.74dB respectively were obtained for Farcha road. This indicates that the highest path loss occurs on Farcha Road while the lowest occurred on Moursal road.

The standard deviation values of 161.27dB, 158.42dB 153.12dB and 151.50dB were obtained for Farcha Road, Digual Road, Moursal Road and Chagoua Road respectively shows that the path loss predicted does not differ significantly.

CHAPTER FIVE

CONCLUSIONS AND RECOMMENDATIONS

5.0 INTRODUCTION

This chapter provides a summary of the results obtained as well as their significance and applications. This is followed with limitations, definition of problems encountered and the solutions proffered to solve these problems. It rounds off with conclusions and recommendations for further work.

5.1 SUMMARY OF RESULTS

In this investigation, it was discovered that spatial particle density increases when the temperature increases. The significance of the increment of dust density is that, when the temperature increases and the pressure decreases this causes the movement of wind, which serve as a means of transporting the dust particles into the atmosphere. In the month of October the particle density value is lower than the months of harmattan. This means that during rainy seasons the amount of dust in the atmosphere drops. While specific particle attenuation variation increases with the size of the dust particle (compared with a wavelength) as well as spatial particle density, and depends on the complex permittivity of the dust particle.

It is found that atmospheric losses display a similar pattern in all cases. The difference, however is that there is a shift in corresponding values of the loss depending on the visibility figure as well as the value of the corresponding wavelength. Atmospheric losses are caused by scattering because the wavelengths of GSM frequencies are larger

than particles size parameter. It is found that particle density in the atmosphere has effect on signal strength. Taking into account the micro size of particles present in the harmattan dust, and on the other hand, the quite high density of fog, the dust particles that cover the atmosphere can be considered as a dielectric. This is because in transmission of signals, dust particles act as interference since they cause loss in electromagnetic energy level of the signals.. On all the sample of roads under investigation, for the network considered the path loss display fluctuation between 59.5dB and 167.5dB between March and January. These variation of path loss and received power can be explained by the increase of dust particles in the air

5.2 SIGNIFICANCE OF RESULTS AND APPLICATIONS

The results of this assessment have relevant application on design in the region, and in the following areas:

- Serve as design guide for radio planners to a thorough understanding of microwave propagation in the region for designing point – to –point links among other things;
- It will give an insight into the propagation characteristics of the harmattan period.
- Monitoring of the radio signals
- Measurements of the field strength
- Fading characteristics and analyses
- Calibrating communication devices.

5.3 LIMITATIONS, PROBLEMS ENCOUNTERED AND SOLUTIONS PROFFERED .

Main limitations confronted in the course of this assessment were:

- Unavailability of field strength measurement data from transmission sites posed a serious problem. Thus use had to be made of the data obtained from staff in the establishment. This was greatly time- wasting as these data could not be obtained in good time and was also responsible for the delay in completing the assessment;
- Unavailability of sophisticated communication equipment to be used for the measurement data. This necessitated the method adopted in this work. Consequently, this limited the number of samples and the accuracy of the measurement data used; and
- Lack of a device that could be used to ascertain the BS transmitter power over the period of harmattan. The measurements were being taken therefore, the transmitter power of celtel was assumed to be constant.

5.4 CONCLUSION

The subject of this thesis has been an assessment of the impact of harmattan particles on microwave propagation in the savannah region. The particle rate (or density) of harmattan dust in the air, specific particle attenuation and atmospheric losses were analyzed and computed. From field strength measurement, the path losses in a typical case were discussed. It can be stated that the objectives for which this investigation was embarked upon have been achieved. It is established first, that the particle density are responsible for scattering electromagnetic energy which can lead to attenuation to its

signal strength. The second atmospheric losses and path losses computed from field strength confirm that particle density does affect signal strength and finally, it is important to state that, due to the limitation highlighted above the results obtained in this assessment are preliminary. More investigation that takes care of these limitations should be conducted in order to improve these results.

RECOMMENDATIONS FOR FURTHER WORK

Throughout this assessment, harmattan effects on microwave propagation were investigated and analysed. These included as a main aim, its effect on the variation of field strength of the signal. “Rate of fading” was not deeply examined but it is felt that further analysis of this phenomenon would be advisable. The speed of fading also can be further analysed in terms of the fading frequency “power spectrum”. This would however require sophisticated equipment.

Another area for investigation of local conditions on microwave propagation could be comparative studies of harmattan effects on different kinds of modulation. This would be interesting. The paramount aspect of the examination of physical phenomenon for instance harmattan, with regards to its influence on radio reception should be conducted on long term basis. For further analysis it is preferable to use two different methods of measuring the field strength not only by using a communication receiver. The second could be based on the use of an electric field strength meter specifically designed for this kind of task. It would be advisable for a radio planner in the savannah region to reduce the distance between BTS’s to avoid the call drops during harmattan.

Some other environmental factors that affect signal propagation should further be investigated.

REFERENCES

1 .Dajab, "Characterisation and Modelling of 900MHz Indoor Wireless communication channels in the savannah region", PhD. Dissertation, Electrical Eng. Dept. Ahmadu Bello University, Zaria 2005, (pages 45-52; 144-152)

2 Chad-Atlapedia Online, Map of Chad-map- zone, 2003. http://cc.msnscache.com/cache.aspx

3. Neyman, A.B "Study of short wave reception in Zaria" PhD dissertation, Electrical Engr Dept. A.B.U ,1981(pages 1-2; 62-63)

4. W.P Callister Jr, "Materials Science and Engineering" An Introduction 4th ed, John Wiley and sons, 1997. New York, 1969.

5. R.H Clarke and John Brown " Diffraction theory and Antennas" Ellis Horwood Limited, England, 1980.

6. M. Dolu Khanov, " Propagation of Radio ware" Miler publishers, Moscow, 1971.

7. H. Frohlich, "Theory of Dielectrics" Oxford university press, 1949.

8. .Ingvar Henne, per Thorvaldsen, "Planning of line-sight radio relay system" 2nd edition NERA Telecommunications, 1999.

9. E.V.D Glazier, H.R.L Lamont, "Transmission and ropagation" Her majesty's stationary Office, vol 5, 1958.

10. Frentzeel L.E "Communication electronics" McGraw Hill, Int, Edition Singapore, 1989.

11. Ezekiel, M "Methods of correlation Analysis", 2nd Edition New York, John Wiley, 1941 Chp 12

12. Y.,Le Guer, P. Reghem, I. Petit and B. Stutz, " Experimental study of Buoyant particle Dispersion in Pipe Flow". Journal of chemical Engineering Research and Design, vol 81, No. A9, October 2003, pp:1136-1143.

13 Isaac I. Kim, Bruce McArthur, and Eric Korevaar "Comparism of laser beam propagation at 785nm and 1550nm in fog and haze for optical wireless communications", Optical Access Incorporated 10343 Roselle street San Diego, CA G2121, 2005. (pages 3-10)

14. Danjuma D Dajab, "Perspectives on the effects of Harmattan on Radio Frequency Waves", Journal of Applied sciences Research, INSInet publication November 2006, (pages 1014-1017)

15. Alexandre S. Martinez; A set of basis functions to improve numerical calculation of Mie scattering in the Chandrasekhar sekera representation,14040-901,Ribeirao preto, SP,Brazil, May 24, 2006.

16. .O.E. Eyo, A.I Menkiti, S.O UDO; "Microwave signal attenuation in Harmattan weather Along calabar Akampkpa line- of- sight link calabar- Nigeria"., Turk J Phys,27(2003),(pages 153-160)

17. Halit Eren; "Particle concentration characteristics and density measurements of slurries using electromagnetic flowmeter"., IEEE Transactions on instrumentation and measurement, vol 44,No.3,June 1995.

18. .R.A Hamilton, N.A and J.W Archbold, M.A; "Meterology of Nigeria and Adjacent territory", November 21,1945.

19. Mohamed M. Sayed, "Microwave and millmeter wave solutions" Santa Rosa, C.A 95404 e-mail: mmsayed@ sbcglobal net phone (707)318-5255, 2004.

20. Shittu Waliu Adisa ; “Cellular Mobile Radio propagation characteristics”, M.Sc thesis, Electrical Engineering A.B.U, 2006.

21. A.R Mishra “Fundamentals of Cellular Network planning and optimization” published by John Wiley and sons ltd, 2004.

22. .www.physcs.uc.edu/courses/electrodynamics.

Appendix A

TableA.1: Monthly Temperature for the Year 2004

Months / Temp^{o}C	January	February	March	October	November	December
Minimum	15.5	16.9	21.4	23.1	19.8	16.3
Average	23.6	25.7	29.4	30.0	28.2	24.7
Maximum	33.2	35.2	38.2	39.0	37.9	35.1

Table A.2: Monthly Temperature for the Year 2005

Months / Temp^{o}C	January	February	March	October	November	December
Minimum	14.7	21.8	25.4	22.2	19.5	17.3
Average	22.6	30.1	32.7	29.2	27.6	25.8
Maximum	31.8	39.8	41.3	36.5	37.6	36.2

Table A..3: Monthly Temperature for the Year 2006

Months / Temp^{o}C	January	February	March	October	November	December
Minimum	17.8	21.1	23.1	23.5	18.3	13.6
Average	26.3	29.4	31.1	29.3	26.2	22.5
Maximum	36.7	39.3	40.1	37.5	35.7	32.4

Appendix B

Table B.1: Monthly Visibility for the Year 2004

Visibility	January	February	March	October	November	December
Meters	600	600	300	800	1000	1000

Table B.2: Monthly Visibility for the Year 2005

Visibility	January	February	March	October	November	December
Meters	200	300	800	800	1000	1000

Table B.3: Monthly Visibility for the Year 2006

Visibility	January	February	March	October	November	December
Meters	1000	1000	300	600	1500	800

Appendix C

Table C.1: Monthly record of relative humidity for the year 2004

Months / Temp°C	January	February	March	October	November	December
Minimum	26.2	25.8	19.1	58.4	29.8	28.5
Average	29.1	25.9	18.8	50.6	29.1	27.3
Maximum	20.4	20.2	16.1	50.1	28.1	27.1

Table C.2: Monthly record of relative humidity for the year 2005

Months / Temp°C	January	February	March	October	November	December
Minimum	34.9	29.8	18.9	60.1	29.9	31.9
Average	24.6	22.5	18.2	55.2	29.5	31.7
Maximum	20.8	16.8	17.2	56.2	27.9	27.5

Table C.3: Monthly record of relative humidity for the Year 2006

Months / Temp°C	January	February	March	October	November	December
Minimum	35.1	26.2	19.2	59.9	33.5	35.9
Average	32.1	16.3	17.9	59.8	31.4	33.8
Maximum	16.8	16.9	15.9	59.4	28.1	30.8

Appendix D

Table D.1: Monthly record of dominant wind for the year 2004

Visibility	January	February	March	October	November	December
Wind direction (degree)	360	40	40	40	40	40
Wind speed (m/s)	9	10	14	6	8	7

Table D.2: Monthly record of dominant wind for the year 2005

Visibility	January	February	March	October	November	December
Wind direction (degree)	40	40	40	180	20	360
Wind speed (m/s)	11	10	11	5	7	6

Table D.3: Monthly record of dominant wind for the year 2006

Visibility	January	February	March	October	November	December
Wind direction (degree)	40	40	20	220	40	40
Wind speed (m/s)	7	8	8	6	8	8

Appendix E

Table E.1: Monthly sample means of field strength for November 2005

Distance (km)	Received signal strength (dBm)							
	Moursal Road	Chagoua Road	Farcha Road	Diguel Road	Kabalai Road	AmTokoui Road	Walia Road	Dembe Road
0.1	-97	-63	-104	-73	-64	-81	-87	-97
0.2	-90	-81	-99	-77	-72	-80	-95	-95
0.3	-94	-73	-95	-72	-80	-70	-97	-100
0.4	-78	-77	-88	-77	-86	-89	-92	-97
0.5	-80	-77	-79	-87	-83	-63	-95	-84
0.6	-88	-81	-88	-84	-81	-86	-86	-102
0.7	-75	-81	-95	-81	-78	-82	-90	-97
0.8	-83	-80	-95	-78	-71	-91	-91	-99
0.9	-84	-85	-96	-74	-85	-95	-88	-99
1.0	-75	-88	-91	-85	-82	-64.8	-83	-99
1.1	-72	-94	-88	-89	-83	-88	-84	-101
1.2	-77	-88	-82	-84	-88	-91	-97	-97
1.3	-76	-83	-79	-81	-65	-88	-98	-99
1.4	-81	-79	-61	-84	-73	-99	-97	-98
1.5	-85	-75	-82	-87	--70	-69.9	-101	-71
1.6	-71	-71	-55	-93	-79	-95	-100	
1.7	-87	-77	-85	-97	-72	-93	-97	

1.8	-80	-74	-47	-98	-91	-97	-103	
1.9	-71	-74	-65	-95	-82	-95	-104	
2.0	-66	-71	-60	-99	-73	-73.0	-70	
2.1	-66	-89	-43	-98	-75	-104	-80	
2.2	-58	-88	-49	-95	-72	-88	-83	
2.3	-60	-77	-50	-93	-74	-94	-98	
2.4	-65	-71	-54	-96	-76	-95	-95	
2.5	-62	-73	-74	-100	-76	-77.1	-90	
2.6	-69	-93	-68	-102	-77	-92	-91	
2.7	-78	-78	-75	-100	-72	-89	-103	
2.8	-86	-80	-72	-101	-74	-89	-87	
2.9	-78	-74	-67	-101	-77	-84	-89	
3.0	-72	-76	-62	-97	-87	-84.5	-95	
3.1	-68	-80	-85	-98	-72	-89	-97	
3.2	-79	-78	-59	-101	-76	-90	-93	
3.3	-71	-72	-86	-102	-70	-85	-99	
3.4	-68	-73	-69	-101	-74	-91	93	
3.5	-66	-62	-90	-100	-75	-90.8	-97	

Table E.2 Monthly sample means of field strength for

January 2006

Distance (km)	Received signal strength (dBm)							
	Mousal Road	Chagoua Road	Farcha Road	Diguel Road	Kabalaye Road	Amtokoui Road	Walia Road	Dembe Road
0.1	-93	-70	-83	-77	-80	-69		
0.2	-86	-81	-75	-82	-69	-47		
0.3	-82	-79	-81	-79	-79	-70		
0.4	-80	-88	-79	-89	-73	-77		
0.5	-85	-68	-78	-80	-53.0	-71		
0.6	-82	-64	-76	-86	-77	-71		
0.7	-78	-59	-82	-86	-71	-75		
0.8	-74	-61	-76	-95	-71	-77		
0.9	-70	-58	-88	-95	-76	-80		
1.0	-57	-70	-88	-90	-55.8	-61		
1.1	-61	-74	-89	-74	-81	-56		
1.2	-65	-73	-93	-78	-71	-58		
1.3	-69	-79	-97	-82	-60	-54		
1.4	-76	-86	-97	-87	-58	-52		
1.5	-83	-93	-98	-81	-58.7	-48		
1.6	-76	-92	-99	-93	-59	-51		
1.7	-75	-97	-99	-94	-58	-65		

1.8	-88	-95	-90	-95	-85	-59		
1.9	-80	-98	-91	-97	-90	-66		
2.0	-80	-98	-93	-97	-61.0			
2.1	-80	-93	-84	-101	-73			
2.2	-79	-90	-80	-96	-84			
2.3	-73	-88	-81	-97	-88			
2.4	-75	-96	-86	-95	-95			
2.5	-82	-93	-86	-99	-74.0			
2.6	-73	-90	-87	-99	-74			
2.7	-69	-89	-73	-93	-78			
2.8	-83	-88	-78	-98	-82			
2.9	-88	-84	-70	-95	-83			
3.0	-72	-83	-70	-89	-80.1			
3.1	-73	-84	-69	-90	-80			
3.2	-72	-87	-61	-82	-77			
3.3	-84	-90	-63	-76	-83			
3.4	-85	-93	-69	-71	-77			
3.5	-67	-88	-73	-89	-92.0			

Table E.3 Monthly sample means of field strength for February 2006

Distance (km)	Received signal strength (dBm)							
	Mousal Road	Chagoua Road	Farcha Road	Diguel Road	Kabalai Road	Amtokoui Road	Walia Road	Dembe Road
0.1	-94	-82	-88	-83	-81			
0.2	-60	-91	-90	-99	-87			
0.3	-94	-91	-87	-98	-78			
0.4	-83	-95	-78	-73	-98			
0.5	-60.1	-80.1	-97	-76	110			
0.6	-95	-95	-87	-83	-89			
0.7	-97	-95	-85	-71	-68			
0.8	-102	-96	-81	-64	-98			
0.9	-103	-99	-75	-78	-98			
1.0	-62.0	-83.0	-86	-89	-89			
1.1	-98	-83	-86	-66	-73			
1.2	-89	-80	-95	-52	-110			
1.3	-93	-81	-86	-47	-96			
1.4	-89	-82	-80	-72	-97			
1.5	-66.1	-83.7	-68	-71	-103			
1.6	-99	-77	-80	-68	-97			

1.7	-92	-75	-84	-70	-100			
1.8	-90	-82	-76	-68	92			
1.9	-82	-80	-78	-54	-88			
2.0	-70.2	-86.0	-62	-60	-101			
2.1	-88	-99	-69	-57	-99			
2.2	-90	-98	-64	-52	-93			
2.3	-90	-97	-75	-60	-104			
2.4	-90	-99	-81	-55	-90			
2.5	-75.1	-88.0	-85	-74	-73			
2.6	-90	-100	-93	-73	-92			
2.7	-95	-100	-80	-76	-99			
2.8	-104	-97	-79	-69	-99			
2.9	-94	-95	-79	-86	-98			
3.0	-82.0	-93.1	-71	-90	-98			
3.1	-94	-99	-85	-75	-104			
3.2	-98	-97	-62	-73				
3.3	-97	-96	-77	-79				
3.4	-88	-99	-77	-79				
3.5	-88	-97	-72	-76				

Table E.4. Monthly sample means of field strength for March 2006

Distance (km)	Received signal strength (dBm)							
	Mousal Road	Chagoua Road	Farcha Road	Diguel Road	Kabalai Road	Amtokoui Road	Walia Road	Dembe Road
0.1	-74	-49	-85	-92	-80			
0.2	-76	-47	-86	-81	-80			
0.3	-84	-50	-88	-84	-82			
0.4	-84	-60	-99	-85	-83			
0.5	-74.0	-61	-49.0	-73	-86			
0.6	-81	-80	-80	-85	-53			
0.7	-77	-74	-84	-93	-87			
0.8	-75	-80	-92	-84	-71			
0.9	-76	-72	-93	-81	-72			
1.0	-83	-70	-55.7	-83	-60			
1.1	-90	-86	-97	-83	-58			
1.2	-87	-77	-98	-75	-59			
1.3	-79	-82	-106	-99	-57			
1.4	-77	-79	-107	-86	-51			
1.5	-84.1	-80	-72.0	-105	-57			
1.6	-71	-59	-95	-98	-58			
1.7	-73	-49	-80	-87	-61			

1.8	-75	-59	-87	-94	-72			
1.9	-65	-53	-88	-90	-72			
2.0	-85.0	-49	-77.1	-90	-74			
2.1	-57	-44	-83	-70	-92			
2.2	-57	-62	-79	-74				
2.3	-61	-70	-80	-45				
2.4	-51	-78	-91	-61				
2.5	-87.0	-85	-78.2	-65				
2.6	-51	-79	-95	-68				
2.7	-79	-80	-102	-67				
2.8	-69	-92	-103	-64				
2.9	-75	-82	-93	-74				
3.0	-90	-78	-84.1	-64				
3.1	-75	-78	-86	-80				
3.2	-74	-75	-87	-72				
3.3	-56	-71	-93	-74				
3.4	-53	-72	-99	-67				
3.5	-95.5	-72	-90	-79				

Table E.5 Measured received signal power and computed path loss for Chagoua road for November 2005.

Distance (km)	Received signal power (dBm)	Computed path loss, Lp (dB)	EIRP (dBm)	Hata model (dB)	Free-space (dB)
0.1	-63	125	62	93.4	71.8
0.2	-81	143	62	103.9	77.6
0.3	-73	135	62	110	81.1
0.4	-77	139	62	114.4	83.6
0.5	-77	139	62	117.9	85.5
0.6	-81	143	62	120.5	87.1
0.7	-81	143	62	122.8	88.5
0.8	-80	142	62	124.9	89.6
0.9	-85	147	62	126.7	90.6
1.0	-88	150	62	128.5	91.6
1.1	-94	156	62	129.7	92.4
1.2	-88	150	62	131	93.2
1.3	-83	145	62	132.2	93.8
1.4	-79	141	62	133.3	94.5
1.5	-75	137	62	134.6	95.1
1.6	-71	133	62	135.4	95.6

1.7	-77	139	62	136.3	96.2
1.8	-74	136	62	137.2	96.7
1.9	-74	136	62	138	97.1
2.0	-71	133	62	139	97.6
2.1	-89	151	62	139.5	98.0
2.2	-88	150	62	140.2	98.4
2.3	-77	139	62	140.9	98.8
2.4	-71	133	62	141.5	99.2
2.5	-73	135	62	142.4	99.6
2.6	-93	155	62	142.7	99.9
2.7	-78	140	62	143.3	100
2.8	-80	142	62	143.8	100.5
2.9	-74	136	62	144.4	100.8
3.0	-76	138	62	145.1	101.1
3.1	-80	142	62	145.4	101.4
3.2	-78	140	62	145.9	101.7
3.3	-72	134	62	146.3	101.9
3.4	-73	135	62	146.8	102.2
3.5	-62	124	62	147.5	103.3

Table E.6 Measured received signal power and computed path loss for Moursal road for January 2006

Distance (km)	Received signal power (dBm)	Computed path loss, Lp (dB)	EIRP (dBm)	Hata model (dB)	Free-space (dB)
0.1	-93	154.5	61.50	93.4	71.8
0.2	-86	147.5	61.50	103.9	77.6
0.3	-82	143.5	61.50	110	81.1
0.4	-80	141.5	61.50	114.4	83.6
0.5	-85	146.5	61.50	117.9	85.5
0.6	-82	143.5	61.50	120.5	87.1
0.7	-78	139.5	61.50	122.8	88.5
0.8	-74	135.5	61.50	124.9	89.6
0.9	-70	131.5	61.50	126.7	90.6
1.0	-57	118.5	61.50	128.5	91.6
1.1	-61	122.5	61.50	129.7	92.4
1.2	-65	126.5	61.50	131	93.2
1.3	-69	130.5	61.50	132.2	93.8
1.4	-76	137.5	61.50	133.3	94.5
1.5	-83	144.5	61.50	134.6	95.1
1.6	-76	137.5	61.50	135.4	95.6

1.7	-75	136.5	61.50	136.3	96.2
1.8	-88	149.5	61.50	137.2	96.7
1.9	-80	141.5	61.50	138	97.1
2.0	-80	141.5	61.50	139	97.6
2.1	-80	141.5	61.50	139.5	98.0
2.2	-79	140.5	61.50	140.2	98.4
2.3	-73	134.5	61.50	140.9	98.8
2.4	-75	136.5	61.50	141.5	99.2
2.5	-82	143.5	61.50	142.4	99.6
2.6	-73	134.5	61.50	142.7	99.9
2.7	-69	130.5	61.50	143.3	100
2.8	-83	144.5	61.50	143.8	100.5
2.9	-88	149.5	61.50	144.4	100.8
3.0	-72	133.5	61.50	145.1	101.1
3.1	-73	134.5	61.50	145.4	101.4
3.2	-72	133.5	61.50	145.9	101.7
3.3	-84	145.5	61.50	146.3	101.9
3.4	-85	146.5	61.50	146.8	102.2
3.5	-67	128.5	61.50	147.5	103.3

Table E.7 Measured received signal power and computed path loss for Farcha road for February 2006.

Distance (km)	Received signal power (dBm)	Computed path loss, Lp (dB)	EIRP (dBm)	Hata model (dB)	Free-space (dB)
0.1	-88	149.5	61.50	93.4	71.8
0.2	-90	151.5	61.50	103.9	77.6
0.3	-87	148.5	61.50	110	81.1
0.4	-78	139.5	61.50	114.4	83.6
0.5	-97	158.5	61.50	117.9	85.5
0.6	-87	148.5	61.50	120.5	87.1
0.7	-85	146.5	61.50	122.8	88.5
0.8	-81	142.5	61.50	124.9	89.6
0.9	-75	136.5	61.50	126.7	90.6
1.0	-86	147.5	61.50	128.5	91.6
1.1	-86	147.5	61.50	129.7	92.4
1.2	-95	156.5	61.50	131	93.2
1.3	-86	147.5	61.50	132.2	93.8
1.4	-80	141.5	61.50	133.3	94.5
1.5	-68	129.5	61.50	134.6	95.1
1.6	-80	141.5	61.50	135.4	95.6
1.7	-84	145.5	61.50	136.3	96.2
1.8	-76	137.5	61.50	137.2	96.7

1.9	-78	139.5	61.50	138	97.1
2.0	-62	123.5	61.50	139	97.6
2.1	-69	130.5	61.50	139.5	98.0
2.2	-64	125.5	61.50	140.2	98.4
2.3	-75	136.5	61.50	140.9	98.8
2.4	-81	142.5	61.50	141.5	99.2
2.5	-85	146.5	61.50	142.4	99.6
2.6	-93	154.5	61.50	142.7	99.9
2.7	-80	141.5	61.50	143.3	100
2.8	-79	140.5	61.50	143.8	100.5
2.9	-79	140.5	61.50	144.4	100.8
3.0	-71	132.5	61.50	145.1	101.1
3.1	-85	146.5	61.50	145.4	101.4
3.2	-62	123.5	61.50	145.9	101.7
3.3	-77	138.5	61.50	146.3	101.9
3.4	-77	138.5	61.50	146.8	102.2
3.5	-72	133.5	61.50	147.5	103.3

Table E.8 Measured received signal power and computed path loss for Diguel road for February 2006.

Distance (km)	Received signal power (dBm)	Computed path loss, Lp (dB)	EIRP (dBm)	Hata model (dB)	Free-space (dB)
0.1	-83	142.5	59.50	93.4	71.8
0.2	-99	158.5	59.50	103.9	77.6
0.3	-98	157.5	59.50	110	81.1
0.4	-73	132.5	59.50	114.4	83.6
0.5	-76	135.5	59.50	117.9	85.5
0.6	-83	142.5	59.50	120.5	87.1
0.7	-71	130.5	59.50	122.8	88.5
0.8	-64	123.5	59.50	124.9	89.6
0.9	-78	137.5	59.50	126.7	90.6
1.0	-89	148.5	59.50	128.5	91.6
1.1	-66	125.5	59.50	129.7	92.4
1.2	-52	111.5	59.50	131	93.2
1.3	-47	106.5	59.50	132.2	93.8
1.4	-72	131.5	59.50	133.3	94.5
1.5	-71	130.5	59.50	134.6	95.1
1.6	-68	127.5	59.50	135.4	95.6
1.7	-70	129.5	59.50	136.3	96.2
1.8	-68	127.5	59.50	137.2	96.7

1.9	-54	113.5	59.50	138	97.1
2.0	-60	119.5	59.50	139	97.6
2.1	-57	116.5	59.50	139.5	98.0
2.2	-52	111.5	59.50	140.2	98.4
2.3	-60	119.5	59.50	140.9	98.8
2.4	-55	114.5	59.50	141.5	99.2
2.5	-74	133.5	59.50	142.4	99.6
2.6	-73	132.5	59.50	142.7	99.9
2.7	-76	135.5	59.50	143.3	100
2.8	-69	128.5	59.50	143.8	100.5
2.9	-86	145.5	59.50	144.4	100.8
3.0	-90	149.5	59.50	145.1	101.1
3.1	-75	134.5	59.50	145.4	101.4
3.2	-73	132.5	59.50	145.9	101.7
3.3	-79	138.5	59.50	146.3	101.9
3.4	-79	138.5	59.50	146.8	102.2
3.5	-76	135.5	59.50	147.5	103.3

Table E.9 Measured received signal power and computed path loss for Diguel road for March 2006

Distance (km)	Received signal power (dBm)	Computed path loss, Lp (dB)	EIRP (dBm)	Hata model (dB)	Free-space (dB)
0.1	-92	151.5	59.50	93.4	71.8
0.2	-81	140.5	59.50	103.9	77.6
0.3	-84	143.5	59.50	110	81.1
0.4	-85	144.5	59.50	114.4	83.6
0.5	-73	132.5	59.50	117.9	85.5
0.6	-85	144.5	59.50	120.5	87.1
0.7	-93	152.5	59.50	122.8	88.5
0.8	-84	143.5	59.50	124.9	89.6
0.9	-81	140.5	59.50	126.7	90.6
1.0	-83	142.5	59.50	128.5	91.6
1.1	-83	142.5	59.50	129.7	92.4
1.2	-75	134.5	59.50	131	93.2
1.3	-99	158.5	59.50	132.2	93.8
1.4	-86	145.5	59.50	133.3	94.5
1.5	-105	164.5	59.50	134.6	95.1
1.6	-98	157.5	59.50	135.4	95.6
1.7	-87	146.5	59.50	136.3	96.2
1.8	-94	153.5	59.50	137.2	96.7

1.9	-90	149.5	59.50	138	97.1
2.0	-90	149.5	59.50	139	97.6
2.1	-70	129.5	59.50	139.5	98.0
2.2	-74	133.5	59.50	140.2	98.4
2.3	-45	104.5	59.50	140.9	98.8
2.4	-61	120.5	59.50	141.5	99.2
2.5	-65	124.5	59.50	142.4	99.6
2.6	-68	127.5	59.50	142.7	99.9
2.7	-67	126.5	59.50	143.3	100
2.8	-64	123.5	59.50	143.8	100.5
2.9	-74	133.5	59.50	144.4	100.8
3.0	-64	123.5	59.50	145.1	101.1
3.1	-80	139.5	59.50	145.4	101.4
3.2	-72	131.5	59.50	145.9	101.7
3.3	-74	133.5	59.50	146.3	101.9
3.4	-67	126.5	59.50	146.8	102.2
3.5	-79	138.5	59.50	147.5	103.3

Table E.10 Measured received signal power and computed path loss for Moursal road for March 2006

Distance (km)	Received signal power (dBm)	Computed path loss, Lp (dB)	EIRP (dBm)	Hata model (dB)	Free-space (dB)
0.1	-74	135.5	61.50	93.4	71.8
0.2	-76	137.5	61.50	103.9	77.6
0.3	-84	145.5	61.50	110	81.1
0.4	-84	145.5	61.50	114.4	83.6
0.5	-81	142.5	61.50	117.9	85.5
0.6	-81	142.5	61.50	120.5	87.1
0.7	-77	138.5	61.50	122.8	88.5
0.8	-75	136.5	61.50	124.9	89.6
0.9	-76	1367.5	61.50	126.7	90.6
1.0	-83	144.5	61.50	128.5	91.6
1.1	-90	151.5	61.50	129.7	92.4
1.2	-87	148.5	61.50	131	93.2
1.3	-79	140.5	61.50	132.2	93.8
1.4	-77	138.5	61.50	133.3	94.5
1.5	-78	139.5	61.50	134.6	95.1
1.6	-71	132.5	61.50	135.4	95.6
1.7	-73	134.5	61.50	136.3	96.2
1.8	-75	136.5	61.50	137.2	96.7

1.9	-65	128.5	61.50	138	97.1
2.0	-61	122.5	61.50	139	97.6
2.1	-57	118.5	61.50	139.5	98.0
2.2	-57	118.5	61.50	140.2	98.4
2.3	-61	122.5	61.50	140.9	98.8
2.4	-51	112.5	61.50	141.5	99.2
2.5	-46	107.5	61.50	142.4	99.6
2.6	-51	112.5	61.50	142.7	99.9
2.7	-79	140.5	61.50	143.3	100
2.8	-69	130.5	61.50	143.8	100.5
2.9	-75	136.5	61.50	144.4	100.8
3.0	-67	128.5	61.50	145.1	101.1
3.1	-75	136.5	61.50	145.4	101.4
3.2	-74	135.5	61.50	145.9	101.7
3.3	-56	117.5	61.50	146.3	101.9
3.4	-53	114.5	61.50	146.8	102.2
3.5	-50	111.5	61.50	147.5	103.3